Geophys. J. Int. (1998) 132, 302–338

Recent crustal deformation in the Antofagasta region (northern Chile) and the subduction process

B. Delouis,[1,*] H. Philip,[2] L. Dorbath[1,3] and A. Cisternas[1]

[1] *Institut de Physique du Globe de Strasbourg, UMR CNRS* JO533, *5 rue René Descartes,* 67084 *Strasbourg, France. E-mail: bertrand@sismo.u-strasbg.fr*
[2] *Laboratoire de Géophysique et de Tectonique, UMR CNRS* 5573, *Université de Montpellier* II, *Place E. Bataillon,* 34060 *Montpellier, France*
[3] *ORSTOM,* 213, *rue La Fayette,* 75480 *Paris, France*

Accepted 1997 August 8. Received 1997 June 17; in original form 1996 November 8

SUMMARY

New neotectonic observations, along with a detailed aerial photograph analysis, allow a new interpretation of the recent tectonic behaviour of the outer forearc in northern Chile between 22.5°S and 24.5°S (Antofagasta region). Both the Coastal Cordillera and the Mejillones Peninsula are under E–W extension. Normal faults dipping east with an almost N–S orientation are predominant. Large-scale Neogene to Recent deformation is characterized by vertical uplift and subsidence related to normal faulting. Recent kinematics along the Atacama Fault System, including the Atacama Fault itself, are controlled by the regional extensional stress regime, and the predominant component of recent displacement along the Atacama Fault is vertical (normal). However, strike-slip components are also observed, but with moderate offsets, no larger than one to two tens of metres. The sense of shear, and the ratio between vertical and horizontal offsets, vary coherently with the fault azimuth, compatible with E–W extension. Oblique-slip faulting, with normal and left-lateral offsets of similar amplitude, is observed on the most northeasterly oriented segment of the Atacama Fault. This small left-lateral component of displacement and the strike-slip motion predicted by models of strain partitioning of the convergence along the Atacama Fault are in opposite senses. This occurs because the stress regime in the coastal region is not compressional but extensional. Very fresh recent ruptures are numerous, especially between 23°S and 24°S, and provide clear indications of the occurrence of moderate to large continental earthquakes during the Late Quaternary. As pointed out by several authors, indirect lines of evidence suggest active subduction erosion and underplating along the margin of northern Chile. We propose that part of the long-term extension is due to the broad-scale flexure of the outer forearc. This flexure may be controlled by offshore subsidence caused by subduction erosion near the trench, and by onshore uplift related to the underplating of eroded low-density material beneath the Coastal Cordillera. Neotectonic observations show that the state of stress in the outer forearc remains extensional (in a deviatoric sense) in the long term. However, it is proposed that the state of stress has a strong time-dependent component, which is intimately linked to the subduction seismic cycle. The $M_w = 8.0$ Antofagasta earthquake of 1995 July 30 showed that large subduction earthquakes produce E–W extension in the coastal region. The overall E–W deviatoric extension in the outer forearc should be reduced by interseismic contraction in the period separating two subduction earthquakes. This reduction means that continental faults will remain locked and aseismic in the interseismic period of the subduction cycle, in agreement with microseismic observations, which indicate an absence of shallow crustal seismicity. We assume that the amount of extension produced by subduction earthquakes in the coastal area is larger than the cumulative interseismic contraction. This occurs because the displacement field generated by subduction earthquakes is concentrated in the outer forearc. The E–W extension should grow over

* Now at: Institut für Geophysik, ETH Hönggerberg, CH-8093 Zürich, Switzerland.

repeated subduction seismic cycles and lead to large continental earthquakes occurring within the overriding block, simultaneous with large subduction events. We show new surface ruptures associated with normal faulting along the Atacama Fault, which were most probably triggered by the 1995 Antofagasta subduction earthquake.

Key words: earthquakes, forearc, neotectonics, northern Chile, subduction.

INTRODUCTION

This paper is primarily concerned with the Neogene to Recent deformation of the Coastal Cordillera in the forearc region of Antofagasta (northern Chile, Fig. 1) and its relationship with the subduction process. The development of the Andes is controlled by the subduction of the oceanic Nazca plate under the South American continent. Due to the short distance (less than 100 km) from the trench to the coast, and to the moderate dip (20°) of the subducting slab above 100 km depth, the coastal area of the present-day forearc region in northern Chile is located only 30–50 km above the coupled part of the subduction plate interface (Delouis *et al.* 1996). As a result, a large part of the continental wedge most strongly subjected to the influence of tectonic movements at the plate boundary is located onshore. Moreover, conditions for the observation of Tertiary to present tectonic structures are exceptional due to the extremely arid climate prevailing on the western margin of the Andes at these latitudes. This makes northern Chile one of the best places in the world for the study of continental tectonics related to subduction. A large $M_w = 8.0$ subduction earthquake which occurred in the Antofagasta region in 1995 helps us to understand part of the interaction between the subduction and the continental deformation.

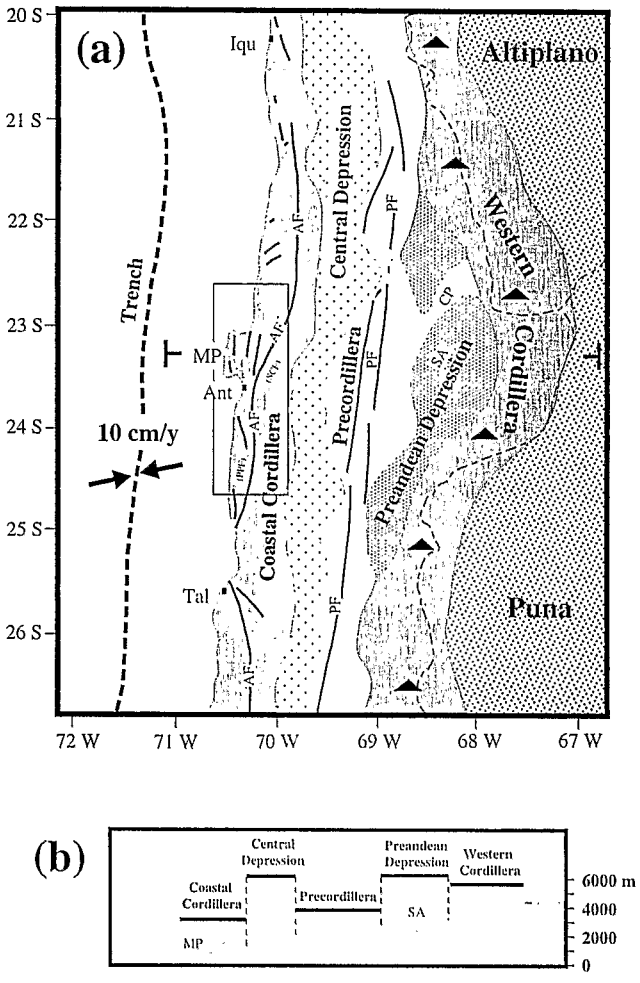

Figure 1. (a) Morphostructural units of the forearc in northern Chile. The different units are described in the text. The volcanic front is located in the Western Cordillera and is represented by black triangles. The frame between 22.5°S and 24.5 S shows the area of study. MP: Mejillones Peninsula; Ant: Antofagasta; Iqu: Iquique; Tal: Taltal; AF: Atacama Fault [(SCF): Salar del Carmen fault segment; (PPF): Paposo fault segment]; PF: Precordilleran faults; SA: Salar de Atacama; CP: Cerros de Purilactis. The position of cross-section (b) is indicated in the central part of the figure. (b) Topographic cross-section at 23.3°S passing through the Mejillones Peninsula (MP) and the Salar de Atacama (SA). Same horizontal scale as (a). The convergence direction is indicated by the double arrow (convergence azimuth and velocity from Pardo-Casas & Molnar 1987).

A major fault zone, the Atacama Fault System (AFS), is present in the coastal range of northern Chile. The origin and evolution of the AFS in the Mesozoic is well established but the nature and geodynamic significance of recent kinematics along the AFS are still a matter for debate. Young normal faulting and E–W extension in the Mejillones Peninsula (MP in Fig. 1) have been recognized by Armijo & Thiele (1990) just north of Antofagasta. These authors also described left-lateral displacements along two SSW–NNE-oriented fault segments (Atacama and Cerro Moreno faults) east of the peninsula. These observations contradict models predicting right-lateral displacements along the Atacama Fault in response to strain partitioning of the slightly oblique convergence, as proposed by Dewey & Lamb (1992). Armijo & Thiele (1990) proposed that a difference in the recent strain regime may exist between the Mejillones block (E–W extension) and the nearby ranges to the east (strike-slip regime), and that the left-lateral slicing along the Atacama Fault zone may be related to the clockwise rotation of the Andean orogen south of the Arica bend. However, the coexistence of normal and left-lateral faulting may be due to the activation of faults of different azimuths under a uniform regional stress regime. To investigate the tectonic regime of the coastal region of Antofagasta further, additional observations along recent ruptures with distinct orientations were needed.

Although much evidence of recent surface faulting has been recognized along the Atacama Fault System (Arabasz 1971; Okada 1971; Armijo & Thiele 1990; present paper), the coastal area, and the forearc as a whole, appear devoid of significant instrumental crustal seismic activity. A permanent telemetric network producing high-quality digital records was installed in 1990 around Antofagasta (23.5°S) by the Institut de Physique du Globe de Strasbourg (France), the ORSTOM (France) and the Departamento de Geofisica of the Universidad de Chile (Chile). It has been shown that seismicity concentrates along the main subduction thrust fault and the Wadati–Benioff zone, and that no superficial earthquakes could be associated with

crustal faults, with the exception of a small cluster located in the deep crust beneath the main branch of the AFS at latitude 23°S (Delouis *et al.* 1996; Delouis 1996). Previous microearthquake experiments in the area led to the same observation of aseismic behaviour of the upper crust (Arabasz 1971; Comte *et al.* 1994).

We contribute new observations and interpretations to the understanding of the forearc tectonics. Aerial photographs as well as satellite SPOT images covering the Coastal Cordillera between 22.5°S and 24.5°S are examined, and the main active faults are mapped. Fault kinematics are studied in the field, and the orientation and shape of the neotectonic stress ellipsoid are found for the Coastal Cordillera. Additional constraints about the Neogene and Quaternary deformation are obtained from marine terraces and other geomorphological data. We analyse both the relatively short-timescale deformation related to individual and repeated seismic cycles and the longer-timescale effect of continuous subduction. Finally, an explanation is proposed for the observed seismic quiescence of the upper crust in the coastal region.

TERTIARY TO RECENT TECTONICS IN THE COASTAL REGION

Background: the Atacama Fault System during the Mesozoic

The Atacama Fault System (AFS) is a continuous fault zone extending over 1000 km in the coastal range of northern Chile between Iquique (20°S) and La Serena (30°S). Recent work between latitudes 20°S and 27°S has established the time of origin of the AFS as Jurassic–Early Cretaceous, that is contemporaneous with magmatic activity in the present Coastal Cordillera (Naranjo *et al.* 1984; Hervé 1987a; Scheuber & Andriesen 1990; Scheuber & Reutter 1992; Brown, Díaz & Grocott 1993). The main branches of the AFZ show ductile sinistral shear zones dated from the Jurassic–early Cretaceous. The AFS would have originated in a transtensional regime produced by the highly oblique convergence between the Aluk (Phoenix) and South American Plates and it would have formed as a trench-linked fault system in the heated and weakened crust of the magmatic arc (Scheuber & Reutter 1992; Brown *et al.* 1993). A transition from ductile to brittle sinistral strike-slip is observed and may have coincided with the cooling of the magmatic arc in the mid-Cretaceous (Brown *et al.* 1993). There is no evidence of Late Cretaceous continuation of the brittle sinistral displacements along the AFS. The Atacama Fault may have inherited its continuous and linear character, which means a steep dip, from its Mesozoic origin as a strike-slip fault.

Cenozoic displacements along the Atacama Fault System

Sense of displacement

Arabasz (1971) and Okada (1971) were among the first who stated that slip on the N–S-trending faults of the AFS must have been predominantly vertical during late Cenozoic times. Arabasz (1971) noted that faulting exerted an important topographic control in the area. In the early work of Okada (1971) the faults bounding the Mejillones high block in the west were considered to be reverse faults. However, Armijo & Thiele (1990) showed that these faults are normal faults. Several authors recognized that faulting along the Paposo segment (24°S–25°S. PPF in Fig. 1) produced uplift of the western side of the fault and closure of west-flowing river valleys (Arabasz 1971; Okada 1971; Mortimer 1980; Hervé 1987b). The formerly continuous ridges and valleys cut by the east-facing fault scarp are not offset horizontally, precluding any significant component of lateral displacement during the recent history of the fault. Further north, Armijo & Thiele (1990) proposed that a difference in the recent strain regime may exist between the Mejillones area and the nearby ranges to the east. They considered that normal faults on the Mejillones Peninsula are indicative of E–W extension, whilst faults east of the peninsula show a significant strike-slip component of motion nearly parallel to the N–S coastline. They reported a predominant left-lateral component of motion along one of the main branches of the AFS northeast of Antofagasta (Salar del Carmen fault segment, SCF in Fig. 1), with a 6 m : 100 m ratio between vertical and sinistral offsets in alluvial fans.

Age of faulting

Hervé (1987b) described a 19 Ma pyroclastic flow in a valley on the western side of the Paposo fault segment, with the source of the flow far to the east. Deposition must have taken place before the closure of the valley, that is before the reactivation of the fault. Furthermore, ash dated at 5.5 Ma was found east of the fault, interstratified within the alluvial fans produced by the erosion of the scarp. Hervé (1987b) concluded that the normal activity along the Paposo segment took place between 19 and 5.5 Ma, that is essentially in the Miocene. Naranjo (1987) pointed out that the southern end of the Paposo segment is truncated by a coastal cliff, which would have been formed before the upper Miocene. Consequently, important vertical motion on the fault would have taken place before the upper Miocene, in agreement with Hervé (1987b). On the other hand, an ash layer dated at 3 Ma is observed on the fault scarp of the Salar del Carmen segment, indicating a more recent age of displacement (Naranjo 1987). Arabasz (1971), Okada (1971) and Armijo & Thiele (1990) reported numerous Quaternary scarps along the AFS and in the Mejillones Peninsula. Arabasz (1971) reported the presence of an offshore fault disrupting the seafloor of the continental shelf in Antofagasta Bay, implying a very recent (Holocene?) age of faulting (Fig. 24c). Neogene normal faulting in the western part of the Mejillones Peninsula is attested by tilting of Miocene to Pliocene marine sediments towards the Morro Jorgino Fault at Caleta Herradura (Armijo & Thiele 1990). With regard to the youngest faulting, Arabasz (1971) reported that together with the extreme aridity, brief periods of torrential rainfall with flooding may occur at intervals of several years, so that it is reasonable to suspect that the age of the youngest faulted alluvium may be up to a few hundred, rather than many thousands of years old.

Field observations

A neotectonic field survey was carried out in April 1995 in the coastal region of Antofagasta (22.5°S–24.5°S). A number of representative sites were selected in order to give an overview

of the fault characteristics and recent kinematics in the area. All sites are located on Fig. 2.

Site 1

The Cerro Fortuna Fault bounds a small westward-tilted block about 1 km wide and 6 km long in its northernmost part. The cumulative east-facing scarp is 60 m high and shows a slope highly smoothed by erosion (Fig. 3). A fresh rupture with a N05°E azimuth and a scarp 1.5 m high follows the foot of this regular slope. Two smaller fresh scarps, 30 cm high, bound a small horst 15 m wide, some 10 m downslope of the main break. Many tension gashes parallel to the scarps may be observed. A subsequent climatic event produced hydrographical incision of the uplifted footwalls of the main rupture and of the newly formed horst. Gullies are observed cutting into the top of the fresh scarps and small alluvial fans spread out downstream. The exposed fault planes present a uniform desert varnish and offset the regular surface of the hillside at a sharp angle. The latter observation suggests that these fresh breaks were produced by a single seismic event. On the other hand, the strong smoothing of the cumulative scarp indicates that the fault must have remained inactive for a very long time. The absence of any evidence of horizontal offset associated with the fault, and the widespread tension gashes trending parallel to the fresh breaks suggest that this last rupture involved pure normal faulting.

We followed the fresh rupture in the field for about 2 km, but it may be traced on the aerial photographs for about 7 km. The main rupture splays into several tension gashes at its southern end, some of them unfilled by sediment, in agreement with a very recent age for this event.

Site 2

Some 35 km south of site 1, another fresh rupture can be observed along the Cerro Fortuna Fault (Fig. 4). Here the fault cuts into detrital formations of probable Neogene to Quaternary age which accumulated in a large west-flowing valley (Quebrada Mejillones) closed by the east-dipping Cerro Fortuna Fault. Although the cumulative scarp in the detrital formation is relatively low, less than 1 m (Fig. 4), natural cross-sections in gullies show that a displacement larger than 10 m occurred on this segment of the fault. The fault is likely to have remained inactive for a long period of time and to have been reactivated recently, at least twice, as indicated by the fresh rupture and the remains of an older, eroded scarp on top of it (Fig. 4).

Site 3

Recent ruptures are numerous along the southern part of the Cerro Fortuna Fault. At site 3 we observed one of the largest fresh scarps of the region, with a 5 m cumulative height (Fig. 5). The exposed fault plane shows only a few traces of erosion.

Site 4

The Morro Mejillones range, in the northern part of the Mejillones Peninsula (Fig. 2), is an uplifted block bounded on its eastern side by an impressive fault, the Morro Mejillones Fault (Figs 6 and 7). The cumulative scarp reaches a height of 400–500 m and shows a complex pattern of faceted spurs and uplifted wave-cut abrasion surfaces. The range front scarp is strongly incised by deep gullies from which emerge several generations of alluvial fans. These fans finally link up with marine sediments of the lowland plain (Mejillones Pampa). This fault was described as a normal fault by Armijo & Thiele (1990), and we focused our attention on the description of the interplay between faulting and alluvial fan deposition at the opening of a large valley (see Figs 7 and 8). The greater height of the scarp observed in the older alluvial fans relative to that observed in the more recent ones (Fig. 7) may be explained by episodic alluvial flow and repeated faulting (Fig. 8). Dating of the cone surfaces would permit an estimation of the displacement rate on the fault. Secondary faults bounding small horst–graben structures are commonly observed downslope of the main scarp. The Morro Mejillones Fault is more active than the fault described at site 1, because the recurrence time between seismic events has not left enough time for erosion to smooth the scarp. No evidence of a strike-slip component could be found, and the presence of tension gashes parallel to the fault in the second (intermediate) generation of alluvial fans confirms that it is a normal fault. We also observed, in April 1995, an open crack on the trace of the main fault in the most recent alluvial fan, which may be the manifestation of a recent seismic event.

The height of the range front scarp decreases towards the south, where the faceted spurs become less well developed. 25 km south of the city of Mejillones (Fig. 2), the scarp completely disappears.

Site 5

The Salar del Carmen fault segment (Atacama Fault) is remarkably continuous over tens of kilometres in the central part of the studied area. The fault bounds a mountain range to the west, and an elongated depression stretches east of it (Figs 2 and 9). This basin–range topography is no doubt strongly controlled by the fault itself. The range stands more than 400 m above its related basin in Sierra Miranda, 40 km northeast of Antofagasta. A detailed examination shows that the fault generally consists of two or more parallel breaks. One fault break is commonly observed at the base of the range and others cut into the alluvial fans spreading out in the basin. The trend of the ruptures varies slightly between N20°E and N30°E. The central parts of Figs 9(a) and (b) include a segment of the Salar del Carmen Fault (Atacama Fault) which has been described by Armijo & Thiele (1990). Armijo & Thiele (1990) presented an interpretive map of the alluvial fan deposits to illustrate the existence of 60–100 m left-lateral offsets along the Atacama Fault. We interpret the correspondence between the fan material on both sides of the fault in a different manner, and, in our opinion, the evidence for the 60–100 m offsets in the alluvial fans is not convincing. Old fans in the footwall west of the fault have been subjected to stronger erosion because they have been uplifted. This differential erosion produced in some cases apparent lateral offsets along the fault. The sense of the apparent lateral offsets is sinistral on the northern sides of the old fans. The southern sides are generally overlain by younger fan material. The systematic deviation of the young fans towards the south reflects the general southward slope of the topography in the area. This deflection is not produced by left-lateral motion along the fault because young

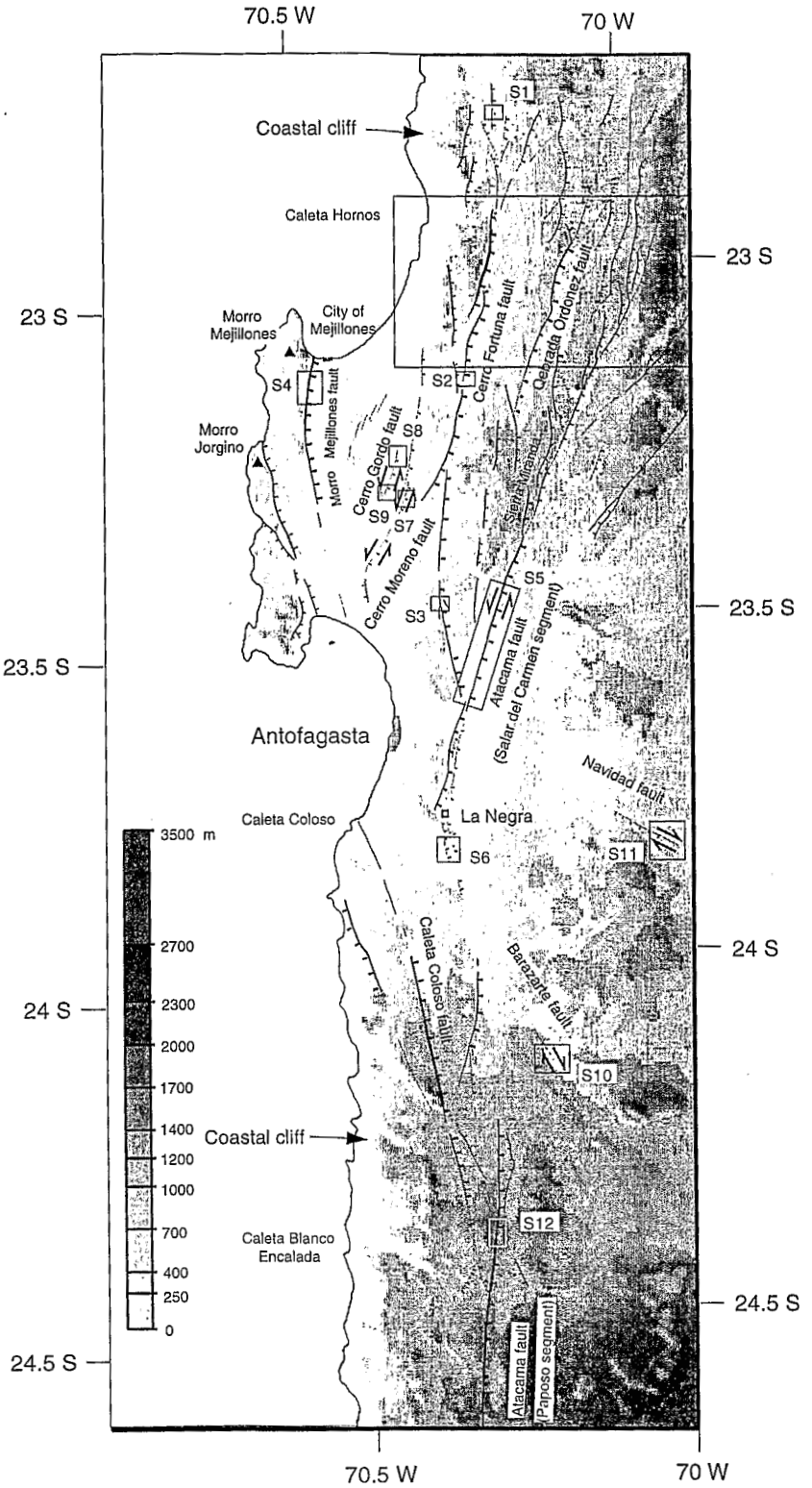

Figure 2. Faults, topography and selected sites in the area of study. Faults were mapped from aerial photographs. Only faults associated with vertical offsets or with lateral offsets observed in the field are drawn. Thickness of line drawing is roughly proportional to scarp height. Thickest lines correspond to cumulative scarps around 500 m high, whilst thinnest lines indicate scarps less than 50 m high. Ticks on the fault traces are towards the downthrow side and indicate normal faulting. When a strike-slip component of displacement is observed, it is indicated by double arrows. Selected sites described in the text are numbered S1 to S12. A large frame around 23 S shows the area where precise topography has been represented in Fig. 25 and where modelling of the topography has been undertaken.

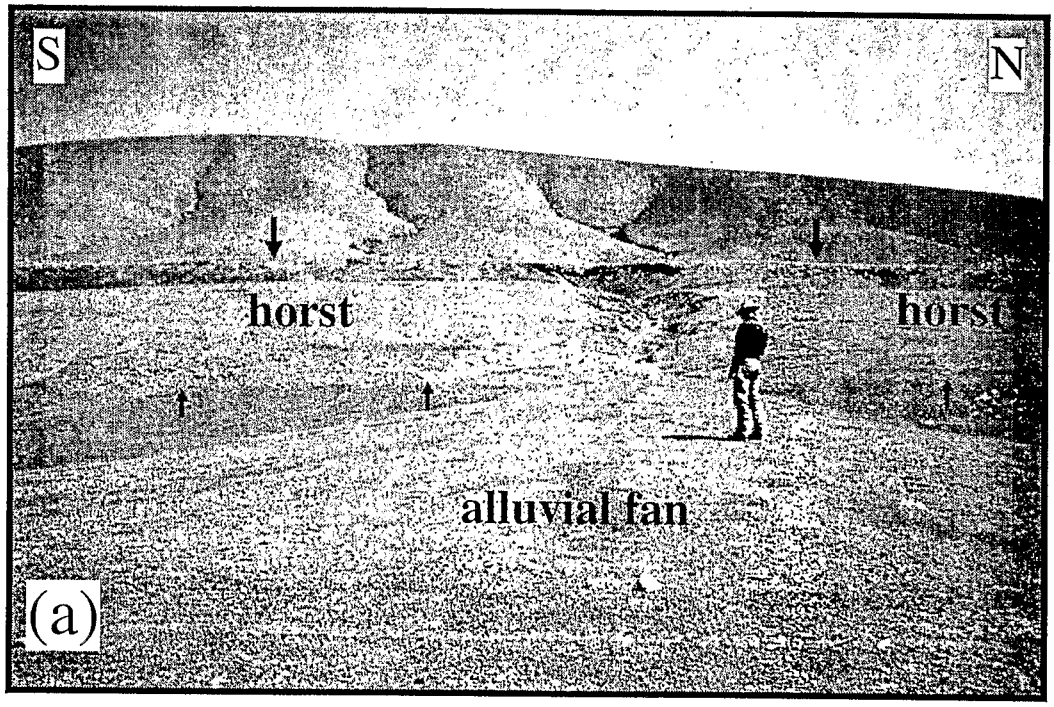

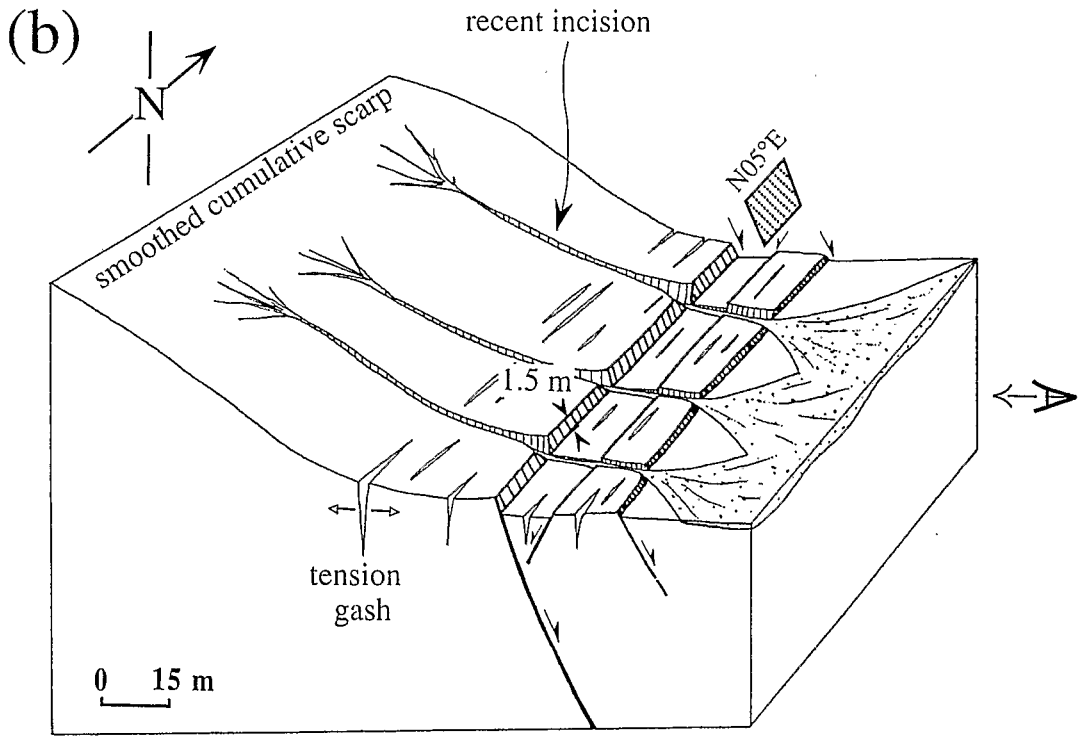

Figure 3. (a) Photograph of a fresh rupture at the northern end of the Cerro Fortuna Fault (see Fig. 2, site S1, for location). The top of the main recent fault scarp, 1.5 m high, is indicated by large arrows. Secondary faults bound a small horst 15 m wide in the hangingwall of the main fault. One of the bounding fault, with a scarp 30 cm high facing to the east, is outlined by small arrows. Note that the main recent scarp is little eroded, except where narrow gullies produced by the last stream incision cut into it. Alluvial fans spread out only after bypassing the horst. Note also the sharpness of the top of the main recent scarp, which may have been produced by a single seismic event. (b) Block diagram showing a complete picture of the recent rupture setting. The arrow and eye indicate the view angle of the photograph (a). Alluvial fans are depicted by dots.

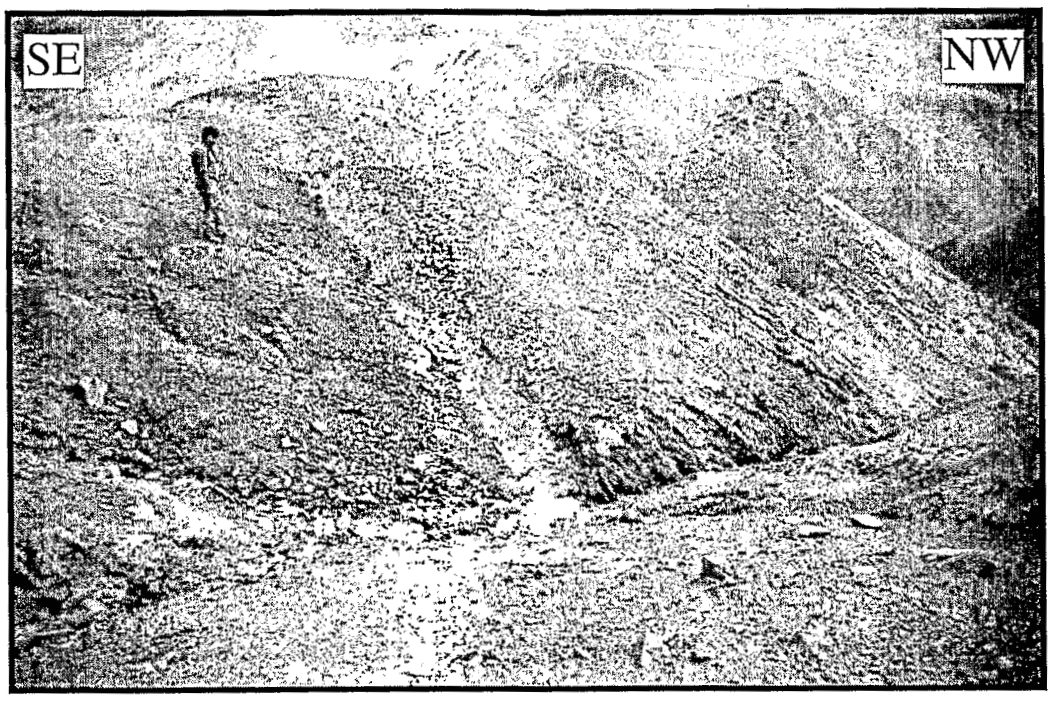

Figure 4. Photograph of a fresh rupture showing normal faulting along the central part of the Cerro Fortuna Fault (see Fig. 2, site S2, for location). Freshness of the scarp is indicated by the light colour of the exposed fault plane. Ridge crests and valleys are not offset laterally by the fault, although the view angle of the photograph does not illustrate this clearly. The fault azimuth is N15 E and dip is towards the east. An older and eroded rupture can be recognized on top of the fresh scarp 60 cm high.

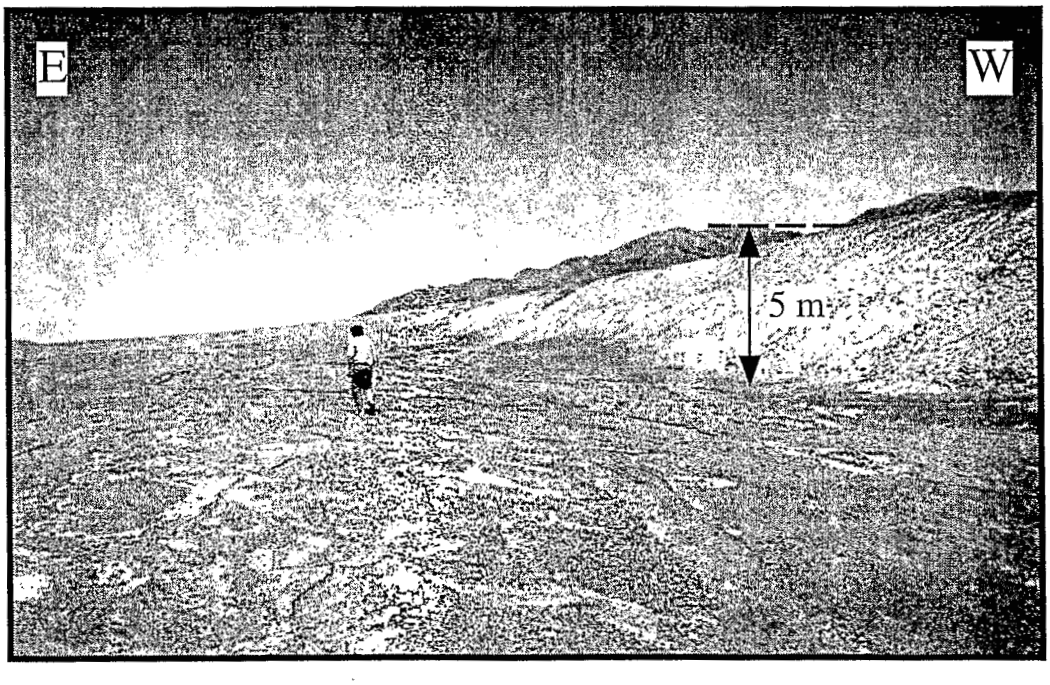

Figure 5. Photograph of a fresh scarp along the southern part of the Cerro Fortuna Fault (see Fig. 2, site S3, for location). Freshness of the scarp is indicated by the light colour of the exposed fault plane. The fault strikes N–S and dips towards the east. The scarp is 5 m high and is apparently very little eroded.

fans are already flowing along the southern wall of the gullies in the uplifted footwall of the fault. In fact, in a number of cases it is observed that the shape of large old alluvial fans affected by the fault is continuous and not laterally offset by the Atacama Fault (Fig. 9).

Armijo & Thiele (1990) also reported several left-lateral stream offsets of a few tens of centimetres to a few metres along the Salar del Carmen segment, although they did not show them. We present here a case of oblique faulting along a small N30 E-trending rupture which confirms the existence

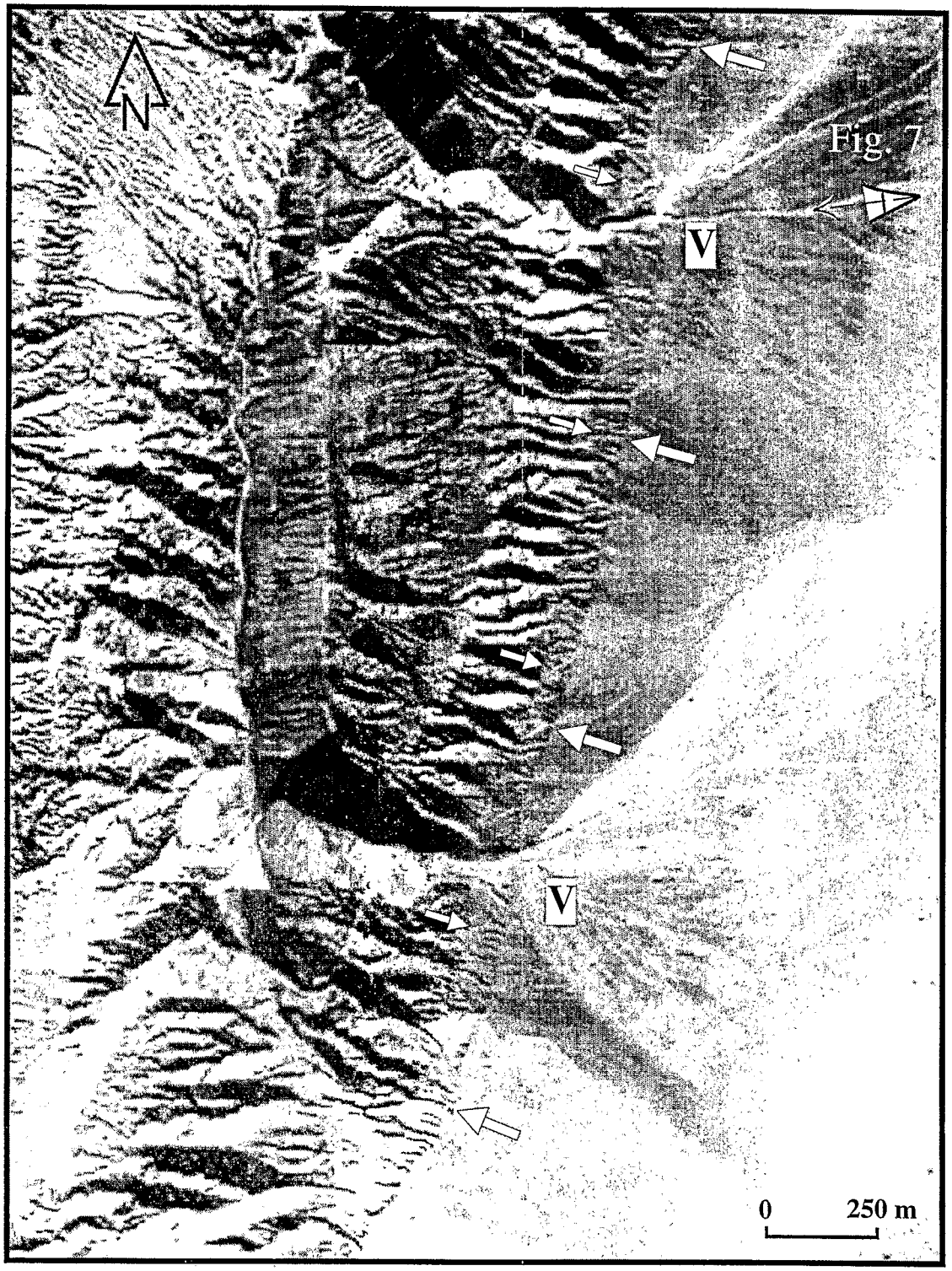

Figure 6. Aerial photograph showing the Morro Mejillones Fault cutting into alluvial fans at the base of the range forming the northwestern highland of the Mejillones Peninsula (refer to Fig. 2, site S4, for location). Large white arrows outline the main fault trace in the alluvial fans, whilst small arrows indicate another fault trace some 100 m upslope. The arrowed eye indicates the view angle of Fig. 7. The two 'V's mark large valley openings.

of moderate-scale left-lateral displacements along the Atacama Fault in this area. A small valley is offset 70 cm vertically and 70 cm left-laterally (Fig. 11). Generally, the undulating surface of the range flank is not significantly offset laterally by the fault, whereas a normal fault offset is clear (for example, see Fig. 10). Ruptures along the range front commonly leave the base of the range to rise on the mountain flank. The main orientation of fresh breaks showing pure normal faulting is N20°E but their orientation may be up to N25°E. Young scarps reach a height of about 8–10 m just north of Antofagasta

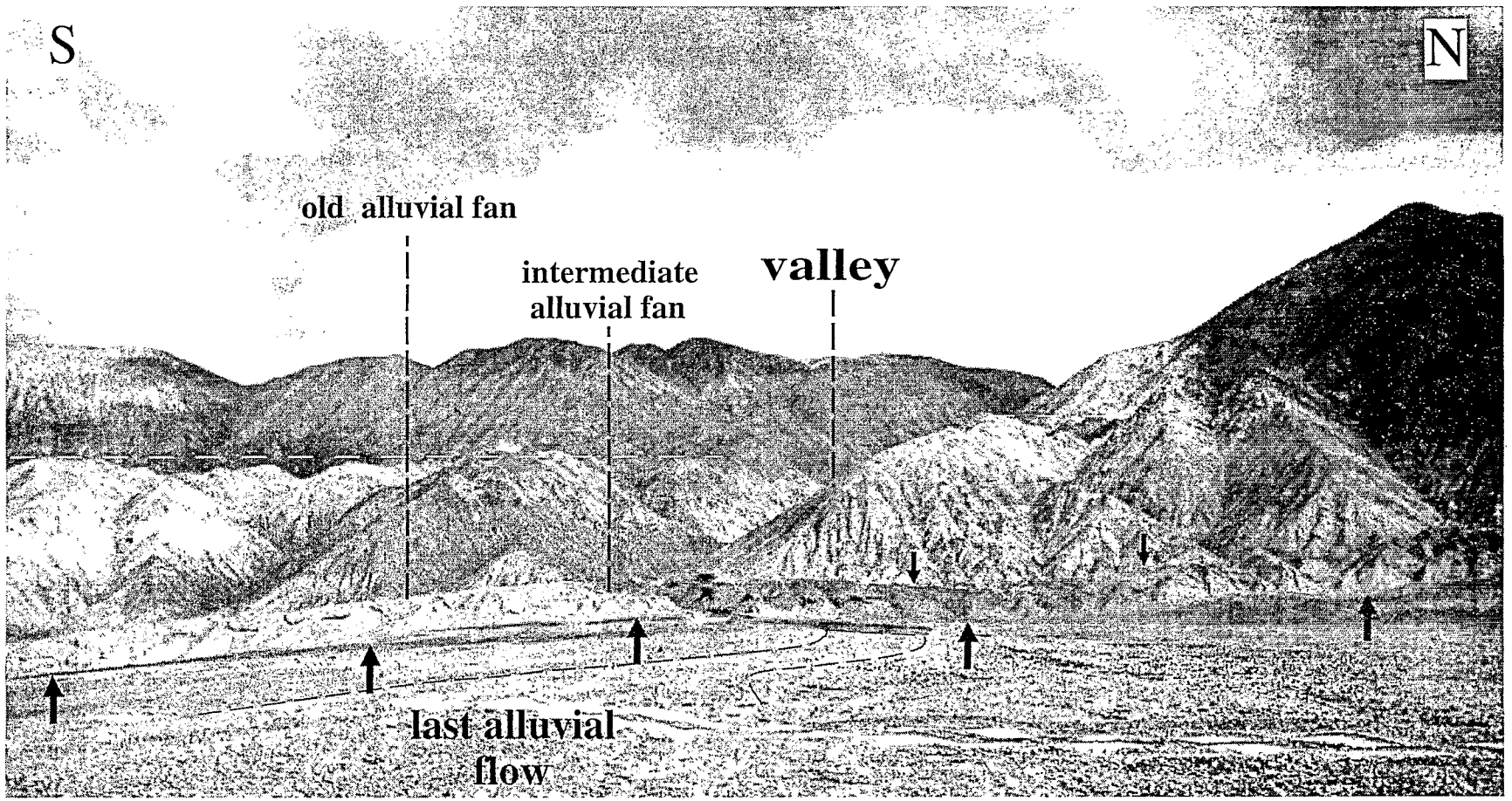

Figure 7. Photograph of the Morro Mejillones Fault at the opening of a large valley (see Figs 6 and 2, site S4, for location). The main fault trace is indicated by large black arrows, whilst smaller arrows outline another fault trace 100 m upslope. Several generations of imbricated alluvial fans can be distinguished. An old, an intermediate-age and a most recent alluvial flow may be clearly recognized. The fault scarp is 8–10 m high in the oldest alluvial fans and 5–6 m high in the intermediate-age fans. Scarps exhibit clear triangular facets formed by erosion. Faceted spurs of triangular form can also be observed along the cumulative scarp of several hundred metres in height. The white dashed line indicates an abrasion surface attributed to marine erosion.

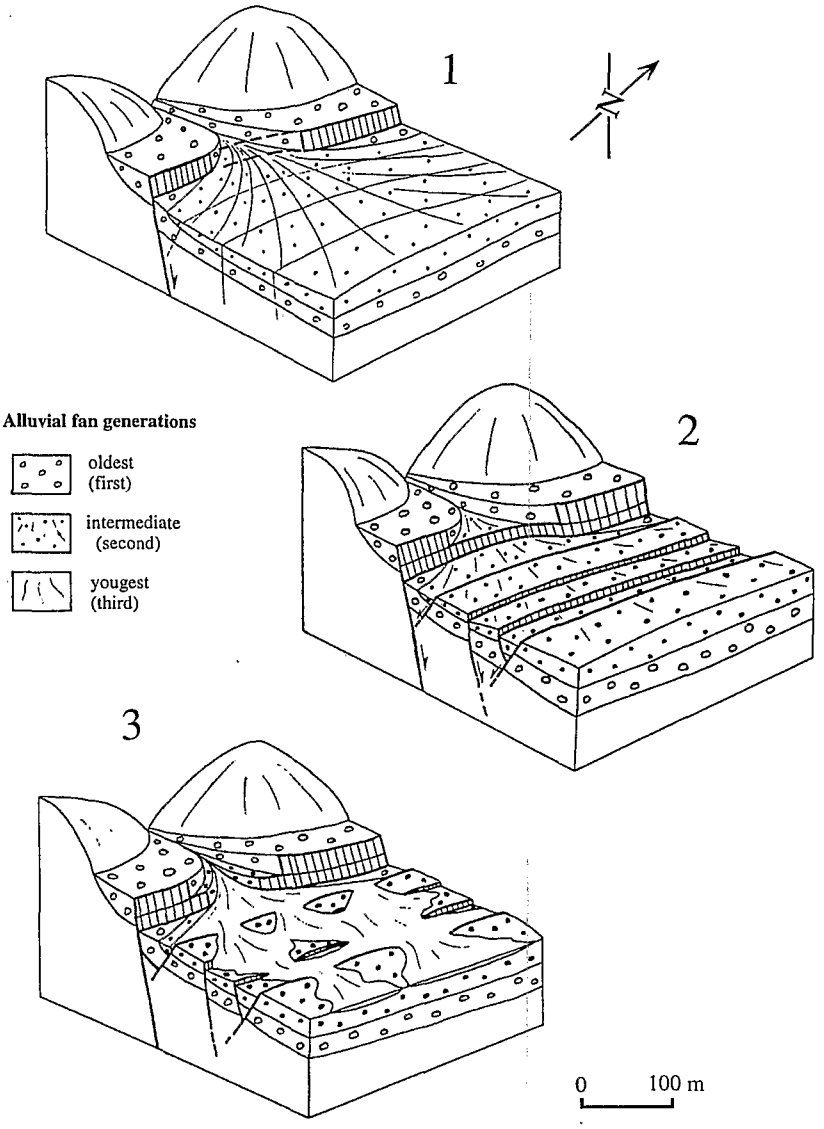

Figure 8. Block diagrams illustrating the interplay between faulting and alluvial fan deposition along the Morro Mejillones Fault. Chronological evolution has been divided into three stages, 1–3. The last stage (3) represents, in a schematic way, the present situation at the opening of a valley, such as those shown in Fig. 6. In stage 1, faulting along the main fault occurred in the intervening time between the emplacement of the first and second generations of alluvial fans. In stage 2, further faulting occurred after the second episode of alluvial fans. Scarp height along the main fault increased and new scarps were created in the hangingwall along secondary faults. In stage 3, the third generation of alluvial fans took place, which eroded existing scarps in several places. Note that scarp height along the main fault is greater in the oldest than in the intermediate-age fans. Further erosion leading to the formation of triangular facets along the main scarp is not shown.

but they are less than 5 m high further north. Downthrow along scarps at the base of the range is systematically towards the east, which is consistent with the topographic high to the west. However, secondary 'antithetic' west-dipping scarps are frequently observed in the alluvial fans (Fig. 9). In some places, where the Atacama Fault seems less active, only the 'antithetic' scarps, acting as dams with respect to the drainage, are visible in the alluvial fans, whilst the east-dipping main scarp is overlain by the fan material.

Site 6

The trace of the Salar del Carmen segment of the Atacama Fault ends south of the 'La Negra' locality, about 20 km SSE of Antofagasta (Fig. 2). Just north of 'La Negra', recent ruptures in alluvial fans reach a height of 10 m or more and the range formed by the footwall of the fault is still 200 m higher than its piedmont. At 'La Negra', the Atacama Fault bends from a mean N20°E trend to the north towards a mean N170°E trend to the south. South of 'La Negra', the fault did not produce any significant relief, and fresh rupture reach a maximum of a few metres. However, ruptures present a very young aspect. Two main fresh ruptures, 1 km apart, lie either within the volcanic 'La Negra' formation (Middle–upper Jurassic), at the contact between the latter formation and the sedimentary 'El Way' formation (Lower Cretaceous) which overlaps it, or within the Quaternary alluvium (Fig. 12). Some features of these fresh ruptures were described by Armijo & Thiele (1990). Topography is not very sharp and consists mainly of an undulating surface sloping gently towards the

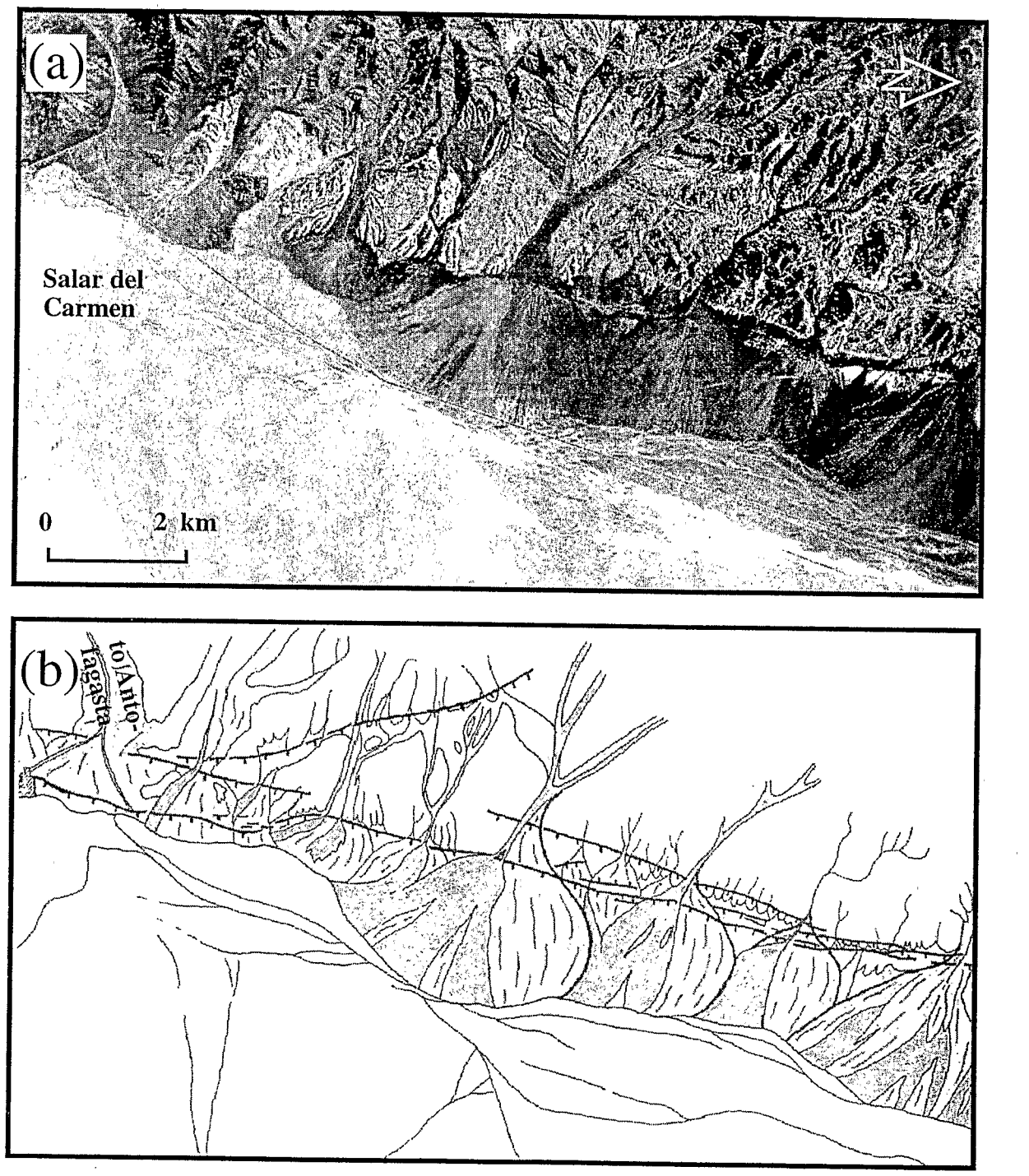

Figure 9. (a) Aerial photograph of the Salar del Carmen fault segment northeast of Antofagasta (see Fig. 2, site S5, for location). (b) Interpretative map. Heavy ticked lines represent the main fault traces with ticks towards downthrow. Two different kinds of alluvial fans are shown in (b), one older (light grey) and one younger (dark grey). Each category of fan does not necessarily form a synchronous family over the whole mapped area because episodic rains responsible for alluvial flows may be very localized in space. Some of the faults displayed in (b) cannot be recognized on the scanned photograph (a) although they were observed on the stereographic view and in the field. (c) Aerial photograph of the Salar del Carmen fault segment north of (a). Locations of Figs 10 and 11 are indicated by boxes. (d) Interpretative map of (c). Fault traces and alluvial fans are represented in the same way as in (b).

east. At some places, the two main ruptures break into en echelon faults or splay into smaller scarps. Large open fissures are frequently observed at the foot of the main scarps. The whole area is hatched by numerous tension gashes which are parallel to the main ruptures. Fig. 13 shows the fault characteristics as it cuts the undulating surface topography. The exposed scarp has a very constant height, even when it crosses small valleys, providing evidence of pure normal faulting. At places

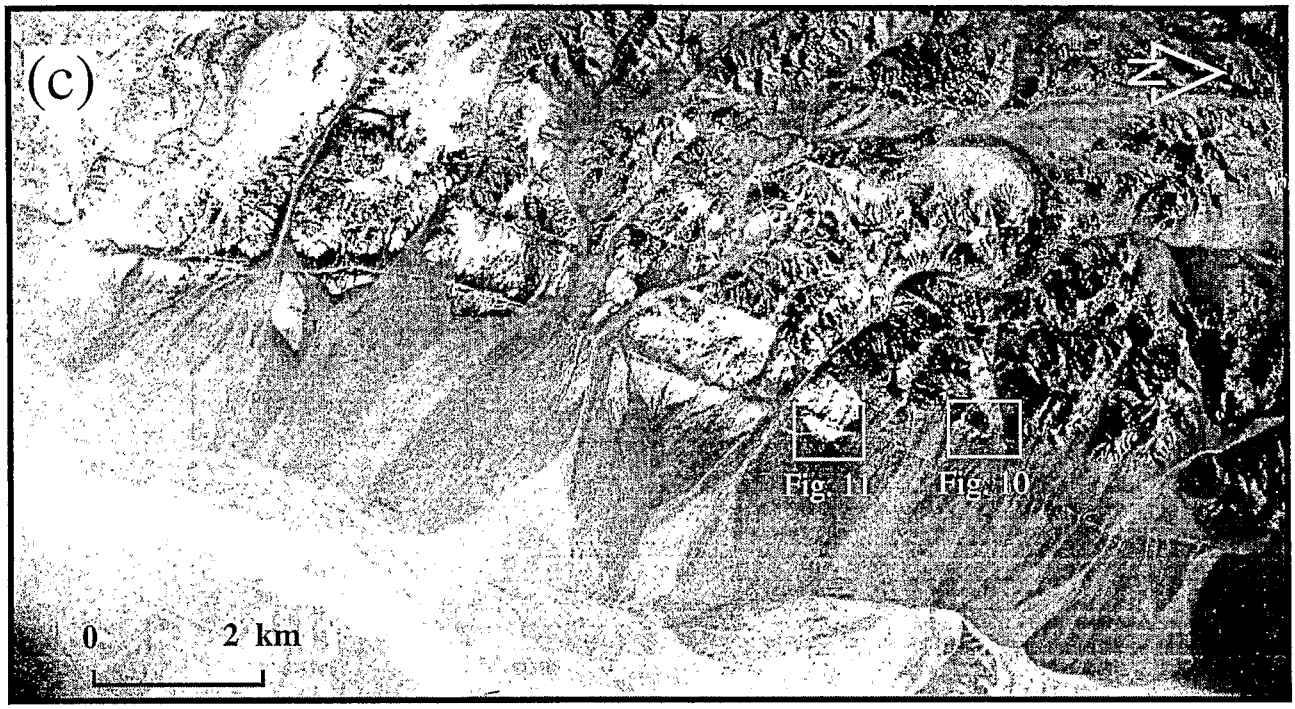

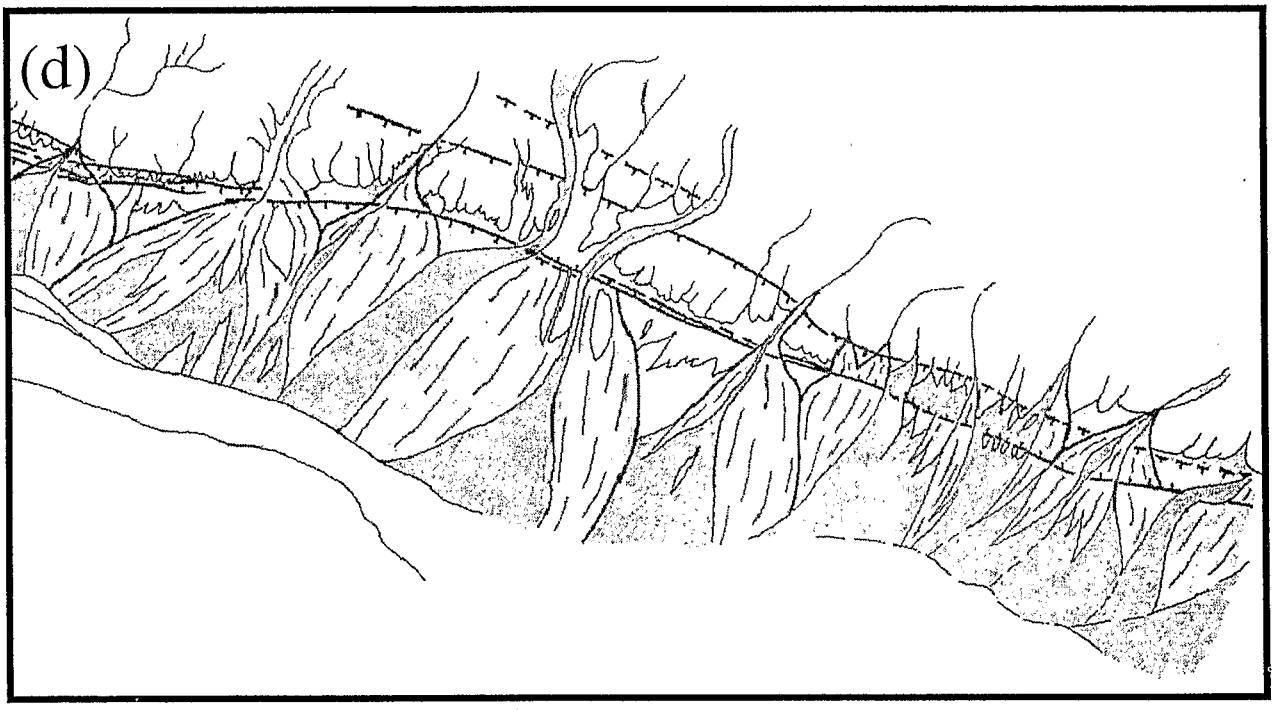

Figure 9. (*Continued.*)

where the rupture crosses large ephemeral stream channels, the scarp has been eroded by the last water flow, and the stream risers are offset in an apparent lateral sense by the fault (Fig. 13b). In fact, this apparent lateral offset, dextral on the southern bank and sinistral on the northern bank, is produced by pure normal faulting. If we closed up the freshest rupture on the main scarps, an older smoothed scarp would remain. This indicates that at least two distinct seismic events produced surface breaking on the fault.

Site 7

The Cerro Moreno Fault has been already described by Armijo & Thiele (1990) as a left-lateral strike-slip fault, with a small normal component. This fault runs on the western border of the coastal range, on the eastern side of the Mejillones lowland. Because the dip-slip component of displacement along the Cerro Moreno Fault is downthrown towards the east, this fault cannot be taken as responsible for the Coastal Cordillera

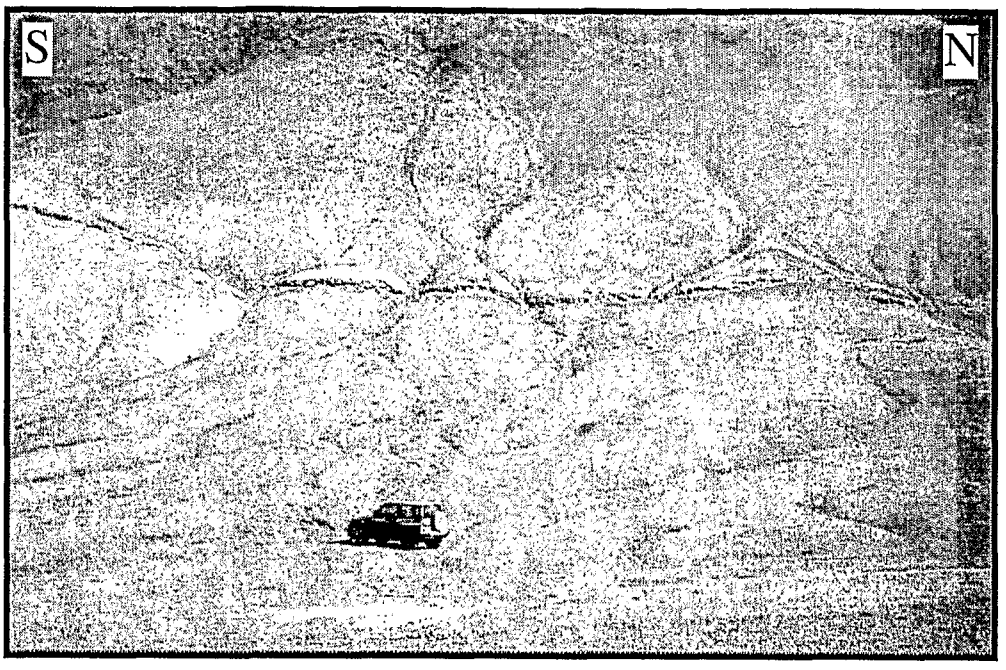

Figure 10. Photograph of one of the fresh ruptures along the Salar del Carmen fault segment northeast of Antofagasta (see Fig. 2, site S5, and Fig. 9c for location). The fault strikes N20 E and dips towards the east. Scarp height is about 1.5 m and lateral offset is insignificant.

relief. Indeed, this fault must be a relatively recent feature cutting the older topography of the coastal range. The relative amplitude of the horizontal and vertical displacement varies with fault azimuth. We observed a ratio of 5 m : 1 m where the fault strikes N30°E and about 3 m : 2 m where it strikes N25°E. For example, Fig. 14 shows a small valley capped with loose gravels displaced 3 m left-laterally and 1.8 m vertically by the N25°E trending scarp of the Cerro Moreno Fault.

Sites 8 and 9

The Cerro Gordo Fault shares many similarities with the Cerro Moreno Fault. It is also located on the eastern margin of the Mejillones lowland, but 2 km eastwards. The fault exhibits oblique left-lateral–normal displacement. As in the case of the Cerro Moreno Fault, the east side is downthrown, and the fault cuts the old topography (site 8, Fig. 15). The east-dipping scarp created by the fault is of metric scale, and acts as a dam for the westerly flowing transient streams coming from the Coastal Cordillera. Small evaporational alluvial basins (salars) are observed at some places east of the scarp. These small sedimentary basins remain after evaporation of the water accumulated in small lakes in drainage sinks against the scarp. The southern termination of the fault takes place on the northeastern flank of the Cerro Gordo mount. Abraded crest surfaces and small gullies observed on the flank are offset 3 m left-laterally and 2 m vertically by the N23 E trending fault (site 9, Fig. 16).

Sites 10 and 11

In the eastern part of the Coastal Cordillera, two active faults with a strike very distinct from the main trend of the Atacama Fault System have been mapped from aerial and SPOT photographs and carefully studied in the field.

The Barazarte Fault (site 10), 50 km southeast of Antofagasta trends N155 E and consists of at least two fault traces about 150 m apart (Fig. 17a). Displacement along the fault is mainly right-lateral, but a small component of vertical (normal) displacement can be observed along some segments of the fault. Fig. 17(b) shows a ridge crest displaced 5 m right-laterally and 0.3 m vertically along one of the fault traces (the one to the west). The top of the ridge was easy to recognize in the field. The second rupture, 150 m away (Fig. 17a), offsets crests and stream channels right-laterally 7–8 m without a vertical component of displacement.

The Navidad Fault (site 11) is the most nearly east–west-oriented active fault identified in the coastal region. It starts 35 km west of Antofagasta and trends N130–140°E (Fig. 18). The Navidad Fault is purely dextral in its eastern part but has a small vertical (normal) component in its western part. Such changes may be related to small variations in fault dip. We carefully mapped part of a recent rupture in the eastern segment of the fault (Fig. 19). Typical features of strike-slip faults are observed along the rupture: en echelon tension gashes, pressure ridges and small pull-apart grabens, all consistent with right-lateral displacement. The vertical component of displacement is insignificant in this part of the fault. Tension gashes are frequently unfilled by sediments. Open cracks cut into recent channels, although not in the most recent ones corresponding to the last water flow. Fig. 20 illustrates the fault attitude in its more western part. There, the Navidad Fault runs along the foot of a small hill range. A fresh rupture shows a vertical offset of 30 cm and a larger, although not precisely measured, lateral offset, which rejuvenated the base of an older smoothed scarp. Pressure ridges between left-stepping en echelon rupture segments and small depressions

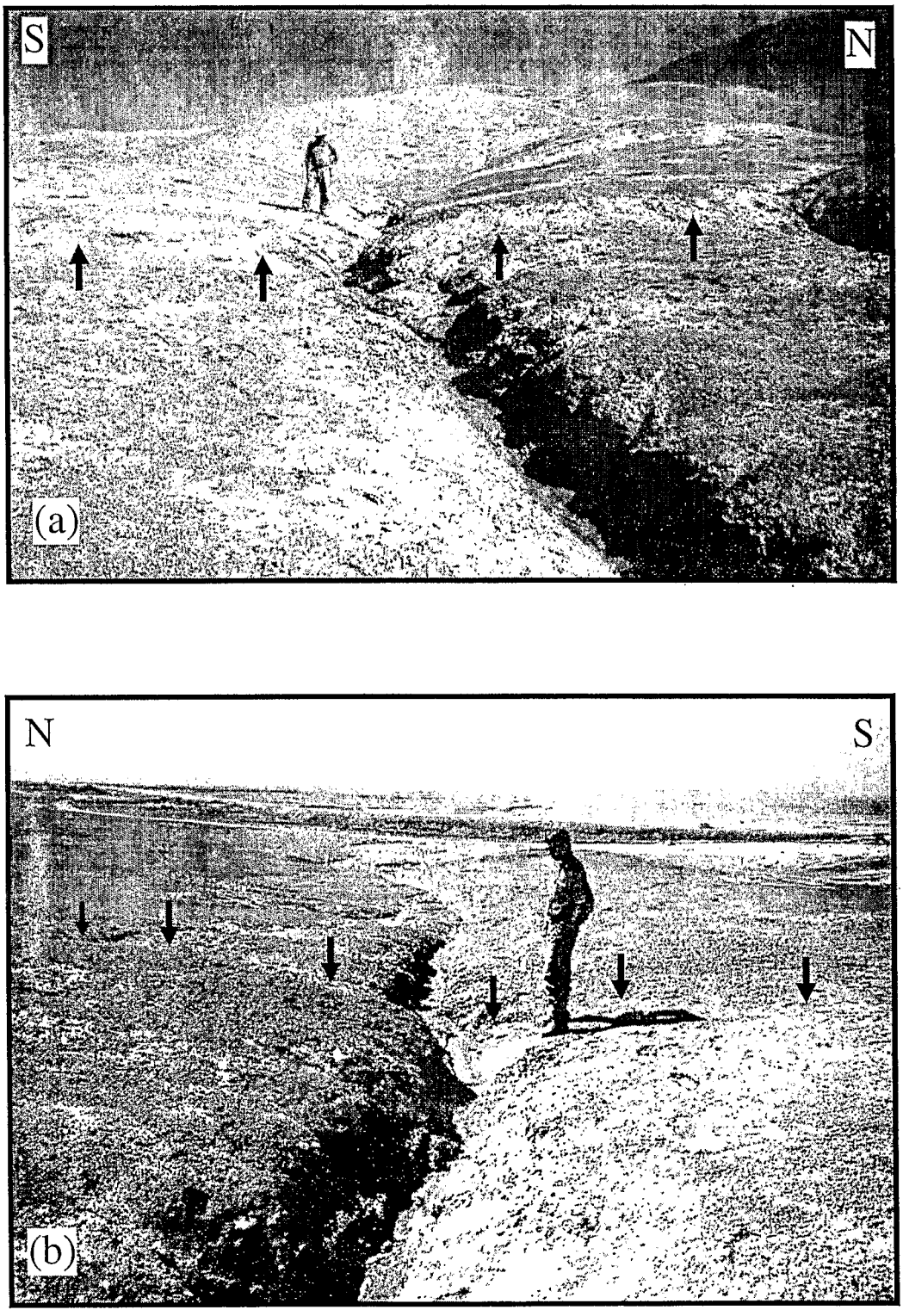

Figure 11. Photographs of one of the fresh ruptures observed along the Salar del Carmen fault segment northeast of Antofagasta (see Fig. 2, site S5, and Fig. 9c for location). The fault strikes N30 E and dips towards the east. Offset comprises 0.7 m of normal displacement and 0.7 m of left-lateral displacement. In (a) the view is to the west. Black arrows outline the base of the scarp. In (b) the view is to the east and the lateral offset can be appraised better. Black arrows show the top of the scarp.

in pull-aparts reveal the dextral component of motion. A small valley bottom capped by gravels offset 13 m left-laterally and 1.3 m vertically gives an example of cumulative displacement. We could not find larger lateral offsets, either on the field or on the aerial photographs.

General statements about field observations

A striking observation is the predominance of east-dipping normal faults over the whole area of study (Fig. 2). In no place, in the field or on aerial photographs, have we found

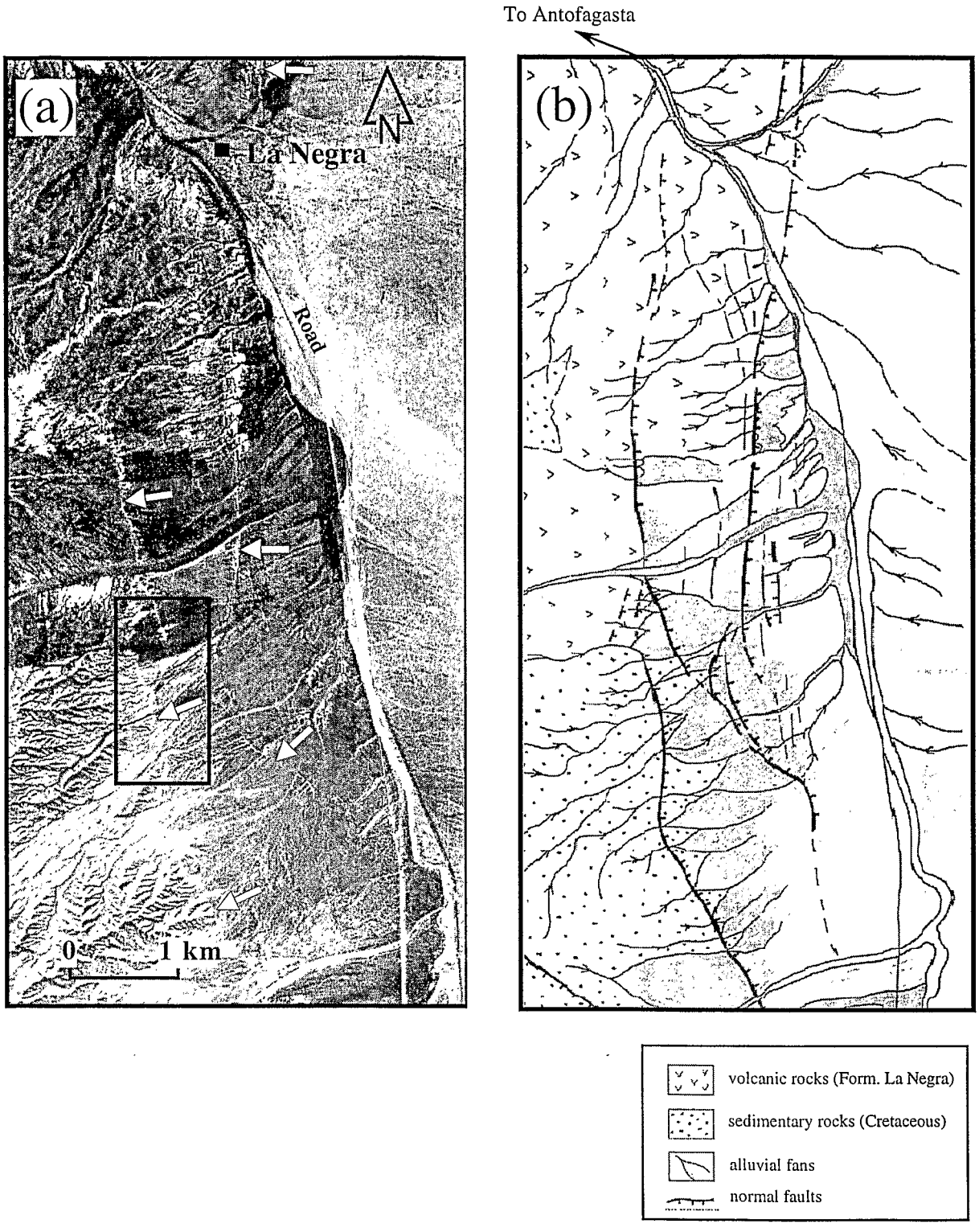

Figure 12. (a) Aerial photograph and (b) interpretative map of the southern end of the Salar del Carmen fault segment, near the 'La Negra' locality (see Fig. 2, site S6, for location). Main ruptures are shown by white arrows in (a). The black box in (a) indicates the area where field observations, described in the text, were made, and where the photograph in Fig. 13 was taken.

evidence of lateral displacements larger than 15 m. It means that no large-scale horizontal block motions, such as those associated with convergence partitioning, are taking place. Deformation is characterized essentially by vertical uplift or subsidence, accompanied by horizontal extension produced by normal faulting. However, although moderate in amplitude, lateral displacements do exist. We found that the sense of lateral displacements, and the relative importance of vertical and lateral offsets, vary coherently with fault azimuth. Although the Atacama Fault System presents an overall

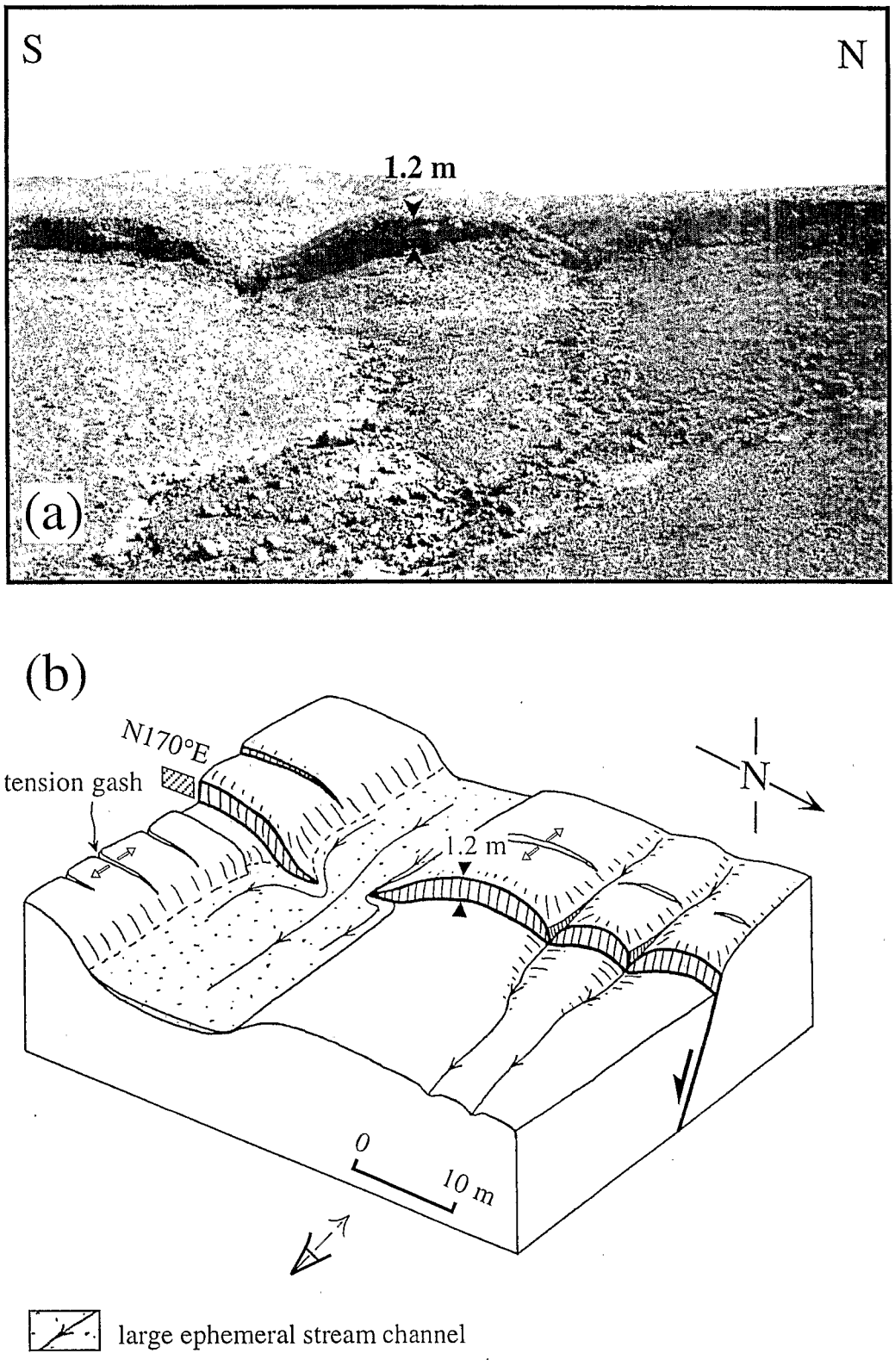

Figure 13. (a) Photograph showing one of the main ruptures observed a few kilometres south of the 'La Negra' locality (see Fig. 2, site S6, and Fig. 12 for location). The height of the fresh scarp is 1.2 m. Scarp height is fairly constant along the fault and small gullies formed before the last rupture are not offset laterally. An older smoothed scarp is observed on top of the fresh one. (b) Block diagram showing the main characteristics of recent faulting in the same area as (a). The arrowed eye indicates the view angle of (a). Note the apparent lateral offset of large ephemeral stream rises due to normal faulting.

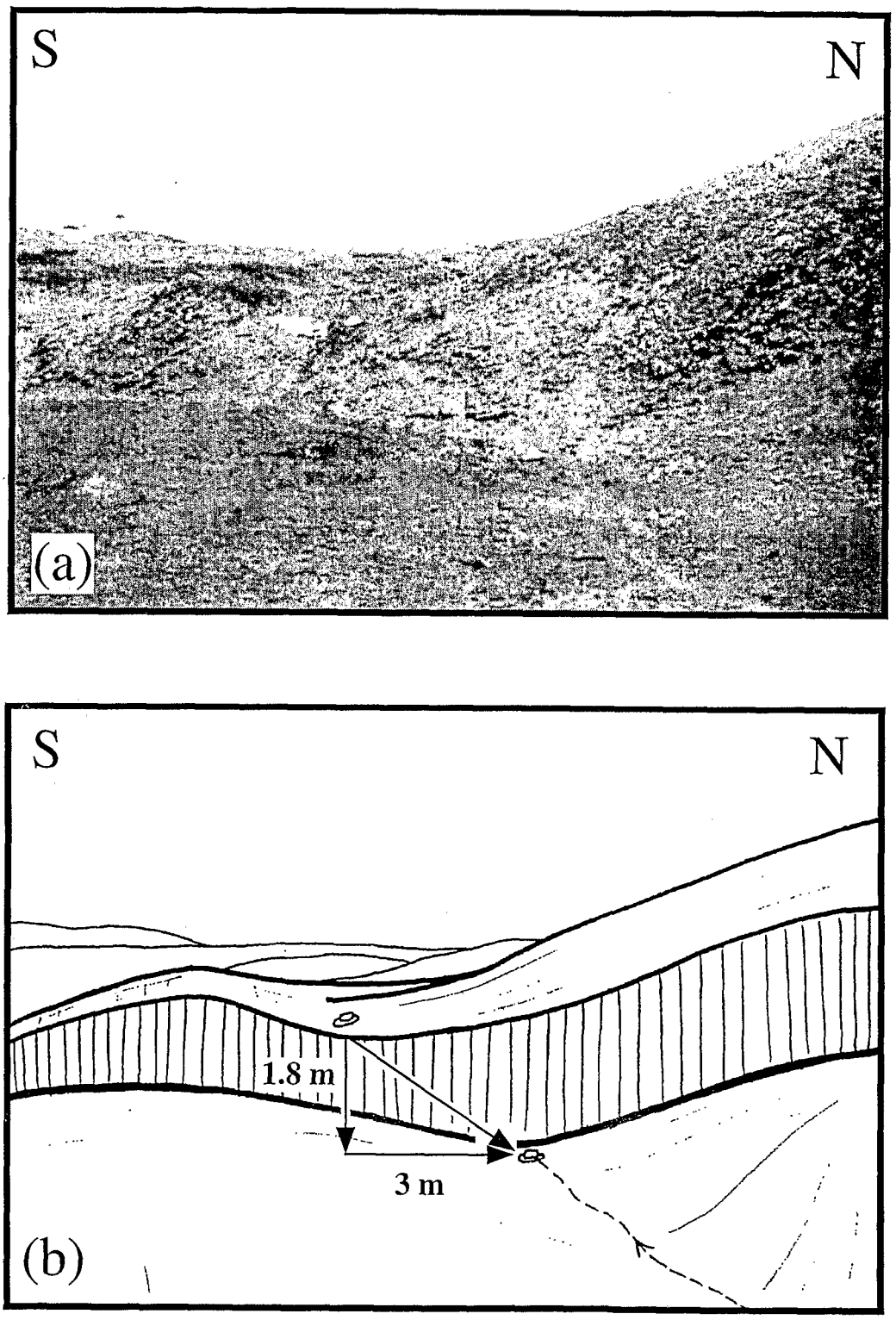

Figure 14. (a) Photograph and (b) sketch of a scarp along the Cerro Moreno Fault (see Fig. 2, site S7, for location). The fault strikes N25°E and dips steeply towards the east. A small V-shaped valley, indicated by the two hats, has been offset 3 m left-laterally and 1.8 m vertically.

appearance of linearity and continuity, Tertiary to Recent fault activity has occurred in a rather segmented fashion when observed in detail (see Fig. 2).

Secondary faults in the hanging wall, especially antithetic faults, are associated with nearly all the large normal faults. In many cases, for instance along part of the Cerro Fortuna and the Salar del Carmen faults, the surface trace of the main east-dipping fault is overlain by fan material and only the antithetic fault can be observed.

From a morphological point of view, several fault segments show the typical shape of old faults with no, or very little, recent activity. This is the case of the Paposo and Coloso fault

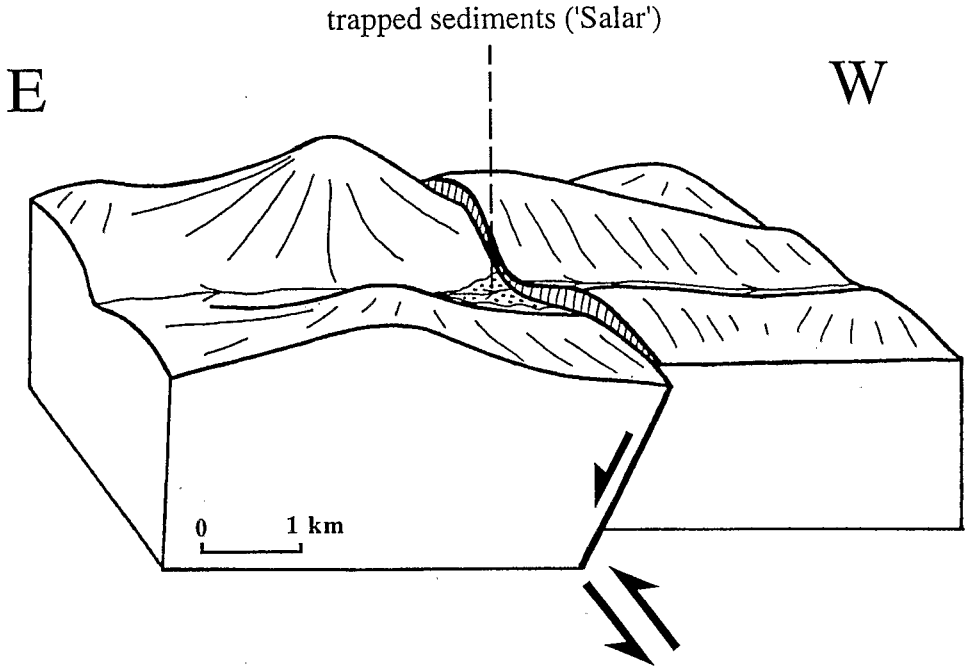

Figure 15. Block diagram illustrating the Cerro Gordo Fault cutting into old topography (see Fig. 2, site S8, for location). Scarp height has been strongly exaggerated for legibility. The fault dips towards the east and exhibits oblique left-lateral–normal displacement. Alluvial sediments episodically flowing towards the west are locally trapped against the scarp and are deposited in small evaporational basins ('salars'). Scale is approximate.

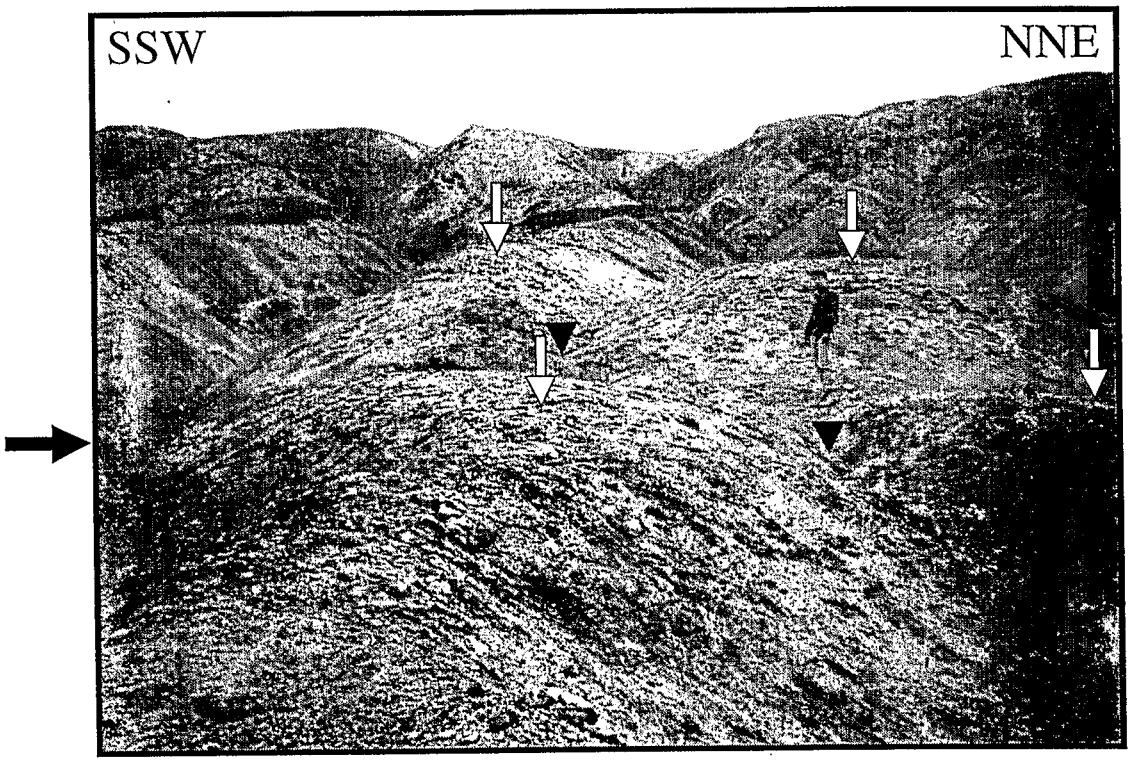

Figure 16. Photograph of the Cerro Gordo Fault on the northeastern flank of the Cerro Gordo mountain (see Fig. 2, site S9, for location). The fault strikes N23°E and dips towards the east. The fault trace is indicated by two black arrows on each side of the photograph. Abraded crests partially preserved (shown by white arrows) were used as reference surfaces to determine the 3 m left-lateral and 2 m vertical offsets associated with the fault. Black arrow heads indicate a small gully offset by the fault.

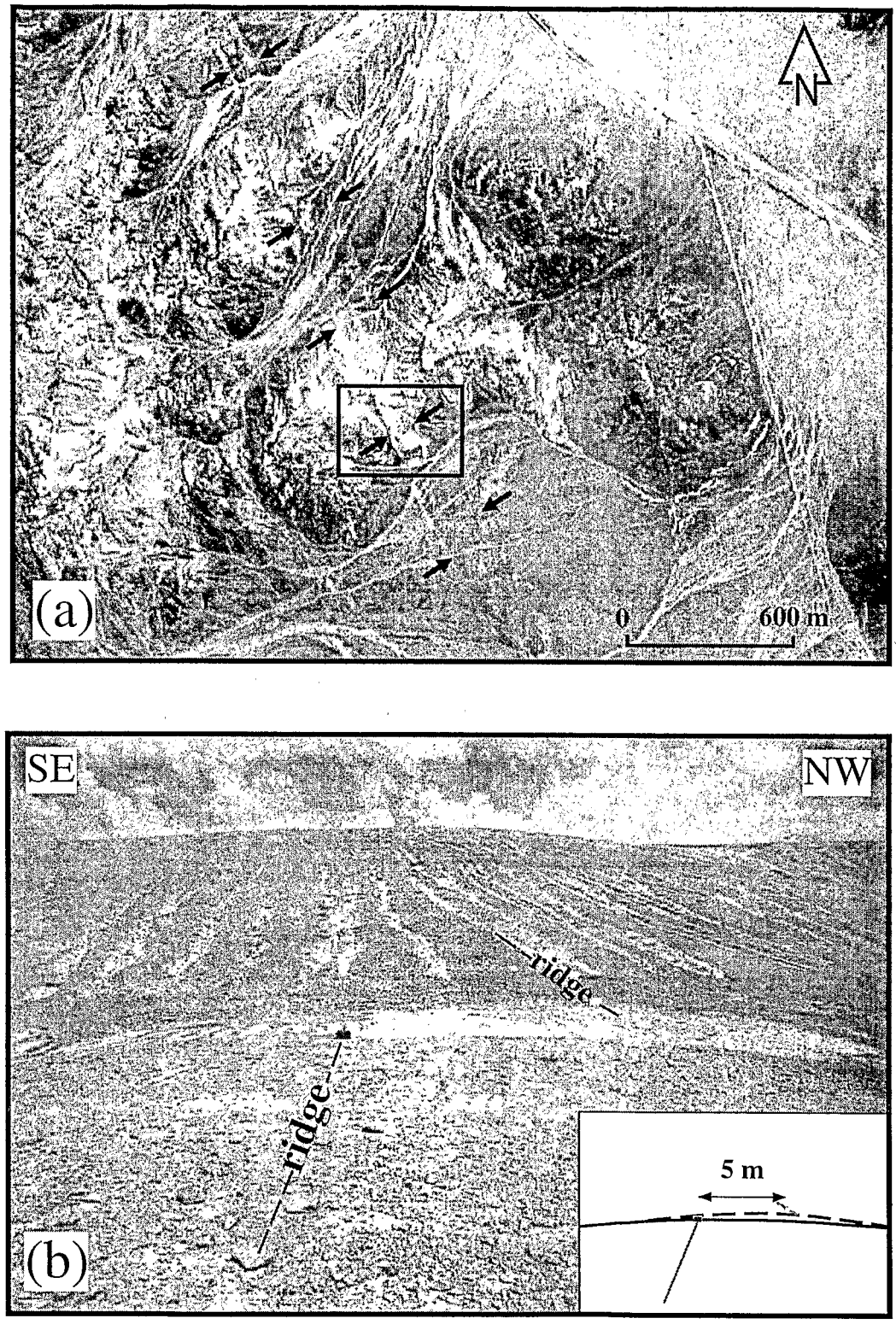

Figure 17. (a) Aerial photograph of part of the Barazarte Fault (see Fig. 2, site S10, for location). Two ruptures, 150 m apart, are outlined by black arrows. Field observations were made inside the framed area. (b) Photograph of one of the ruptures shown in the framed area of (a). A ridge line is offset 5 m right-laterally. A small vertical (normal) component of displacement of about 0.3 m contributed to the scarp height. The fault azimuth is N155°E.

segments (Fig. 2) whose recent inactivity has been documented (Hervé 1987b; Martinez & Niemeyer 1982). The Quebrada Ordoñez Fault (Fig. 2) shows the same morphology and is considered to be currently inactive. Generally, fault segments which achieved a high topographic morphology with cumulative scarps several hundred metres high do not show fresh ruptures and appear to be inactive. This is the case for part of the Cerro Fortuna Fault, around 23°S, and part of the Salar

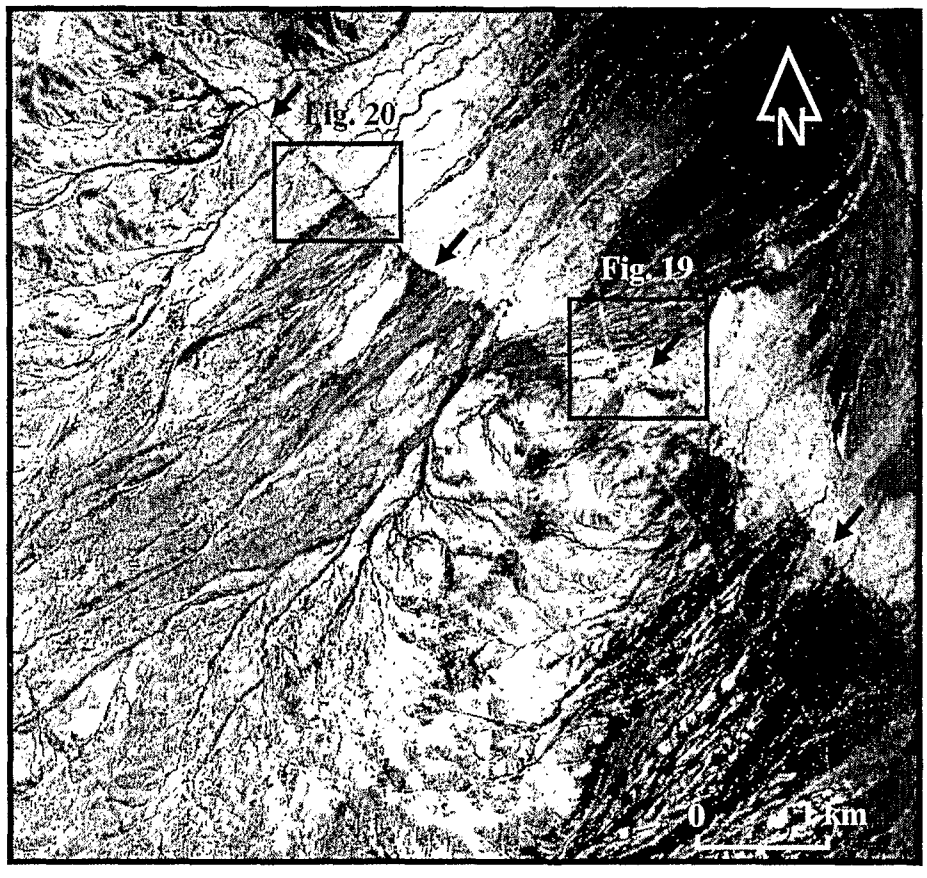

Figure 18. Aerial photograph of the Navidad Fault (see Fig. 2, site S11, for location). Black arrows indicate the fault trace. Although the right-lateral component of displacement predominates all along the fault, the cumulative vertical offset (less than 2 m) is strongly outlined in aerial view due to blocking of alluvial fans. The absence of large lateral offsets may be due to the recent age of fault activation. Boxes indicate locations corresponding to Figs 19 and 20.

del Carmen Fault, between 23 S and 23.5 S (Fig. 2). These are typical cases where only the antithetic faults can be recognized. A notable exception is the Morro Mejillones Fault, with a 400–500 m cumulative scarp, which shows morphological evidence of recent activity in its northern part (site 4). An important observation is that fresh breaks are more frequent in the central part of the studied area, between 23 S and 24 S, i.e. landward, and around Antofagasta and the Mejillones Peninsula, than further south (Paposo Segment) and further north.

Neotectonic stress tensor analysis

Field observations of relative motion along fresh ruptures were used to investigate the stress regime in the Antofagasta coastal area. We used an algorithm of stress tensor determination from observed motions on fault planes. Data are fault strike, dip and slip angles (Aki & Richards 1980) at 12 selected sites (Table 1). The assumption in this method is that the stress tensor does not vary significantly in the area of observations and in the period of time sampled by the fault data. Search parameters are three Euler angles, to define the orientation in space of the eigenvalues of the stress tensor σ_x, σ_y, σ_z and the shape factor $R=(\sigma_z-\sigma_x)/(\sigma_y-\sigma_x)$, with $\sigma_y>\sigma_x$, σ_z being the eigenvector closest to the vertical (Armijo, Carey & Cisternas 1982). The connection between σ_x, σ_y, σ_z and the ordered eigenvalues σ_1, σ_2, σ_3 can easily be established for any R-value. Exploration of the parameter space is carried out by a Monte-Carlo process. The best parameters are selected so as to maximize the sum of the scalar products between theoretical and observed slip vectors. Strikes of fault planes were measured in the field. Observed slip angles were calculated from the ratio between the vertical displacement projected on the fault and the lateral offset. The dip of fault planes was difficult to obtain from field observations, and different values have been tested. The best results were obtained with a dip of 60° for pure normal faults, and a dip between 70° and 90° for oblique to pure strike-slip faults. The 10 best tensors found are shown in Fig. 21. The scatter is low and the stress tensor is well constrained by the data. The stress regime is extensional with σ_1 vertical and σ_3 horizontal, oriented between N89°E and N101 E. The R-factor varies between 0.96 and 1.7, and indicates triaxial extension. Fig. 22 shows the fit between the theoretical (calculated) and observed slip vectors in stereographic projection and in plane view for the best stress tensor. Overall agreement is good, the angular difference between theoretical and observed slip vectors being less than 26°, with an average difference of 12 .

Marine terraces: constraints on coastal uplift and local faulting

The last interglacial maximum eustatic sea-level stand occurred around 125 000 years ago, and at that time, eustatic sea level

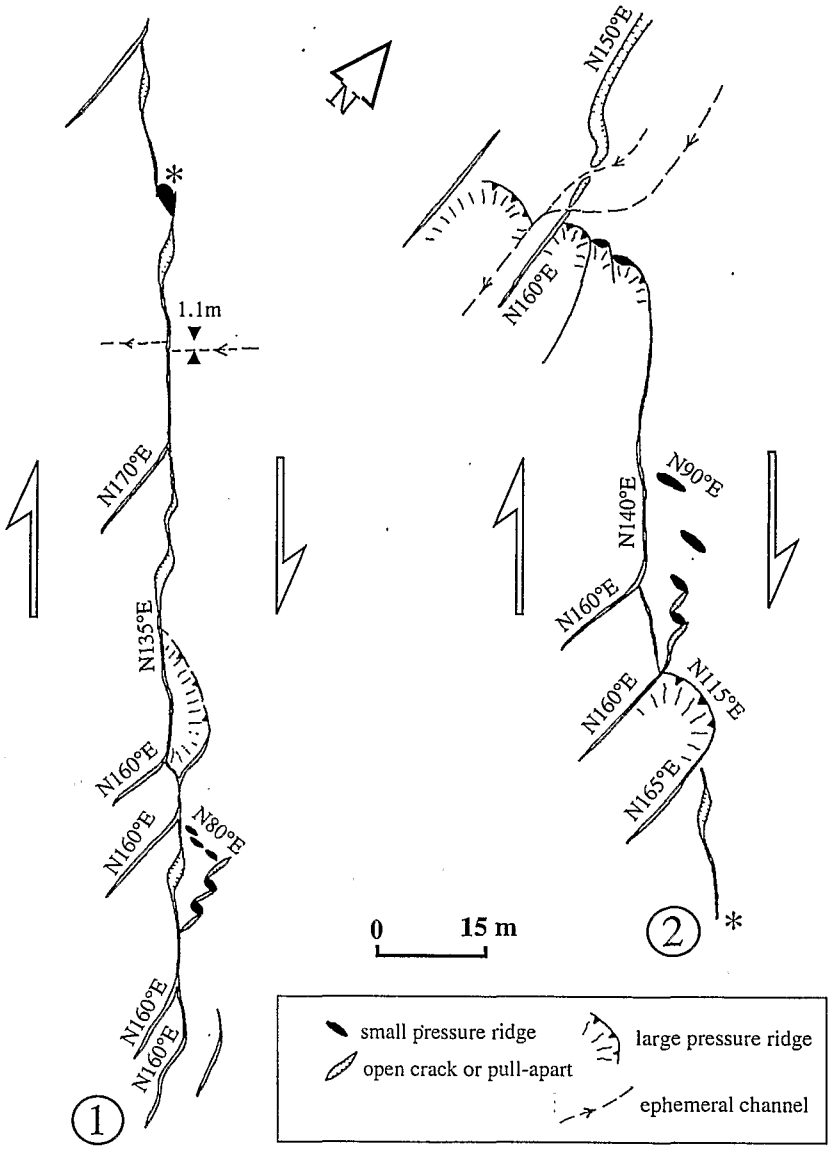

Figure 19. Map of a recent rupture along the eastern part of the Navidad Fault (see Fig. 18 for location). The map has been divided into two parts (1 and 2) slightly overlapping and joining at the star. The fault trace shows a complex pattern of cracks, pressure ridges and pull-apart depressions in agreement with right-lateral shear along the N140°E direction. No vertical component of displacement is observed and the only quantification of lateral offset is given by an ephemeral channel displaced 1.1 m.

was ≈ 6 m above its present height (Leonard & Wehmiller 1991). Terraces formed during the last interglacial have been identified (dated) in a number of places in northern Chile, in particular in and around the Mejillones Peninsula. Fig. 23 shows average uplift rates obtained by several authors for the last 125 000 years, and, in some places, for longer or shorter periods. Maximum bounding values of uplift during Quaternary times were obtained from the height of terraces where upper Pliocene marine fauna were found, assuming a 2 Myr age.

The overall pattern of uplift in the region shows significant variations (Fig. 23). Small average uplift rates for the whole Quaternary characterize the coast in the bay of Antofagasta, and stability or small subsidence is observed on the southern margin of the Mejillones Peninsula (Juan Lopez, Caleta Errazuriz) and in Antofagasta Bay for the last 125 000 years. On the other hand, Quaternary uplift rates of 0.20–0.22 mm yr^{-1} characterize the central part of the Mejillones lowland and the Morro Jorgino–Cerro Bandurria horst block. On the Morro Mejillones, the highest abrasion surfaces (topping the relief) were recently interpreted to be of Pliocene age, and the highest Pleistocene deposits were found at an elevation of 440 m (Ortlieb *et al.* 1996). In the absence of precise dating, the uplift rate of the Morro Mejillones is not well constrained, but values of the order of 0.3 mm yr^{-1} or greater may be proposed. Footwall uplift along the Morro Mejillones Fault is responsible for this localized high uplift, and hangingwall subsidence would account for the relatively low uplift rate (0.07 mm yr^{-1}) observed at El Rincon (Fig. 23). Although the correlation between active faulting and uplift rates is good in this case, the relationship between faulting and the regressive shorelines observed on the Mejillones lowland is not fully explained. Ortlieb (1993) noted that the very regular spacing of the regressive shorelines, which cover most of the Pleistocene,

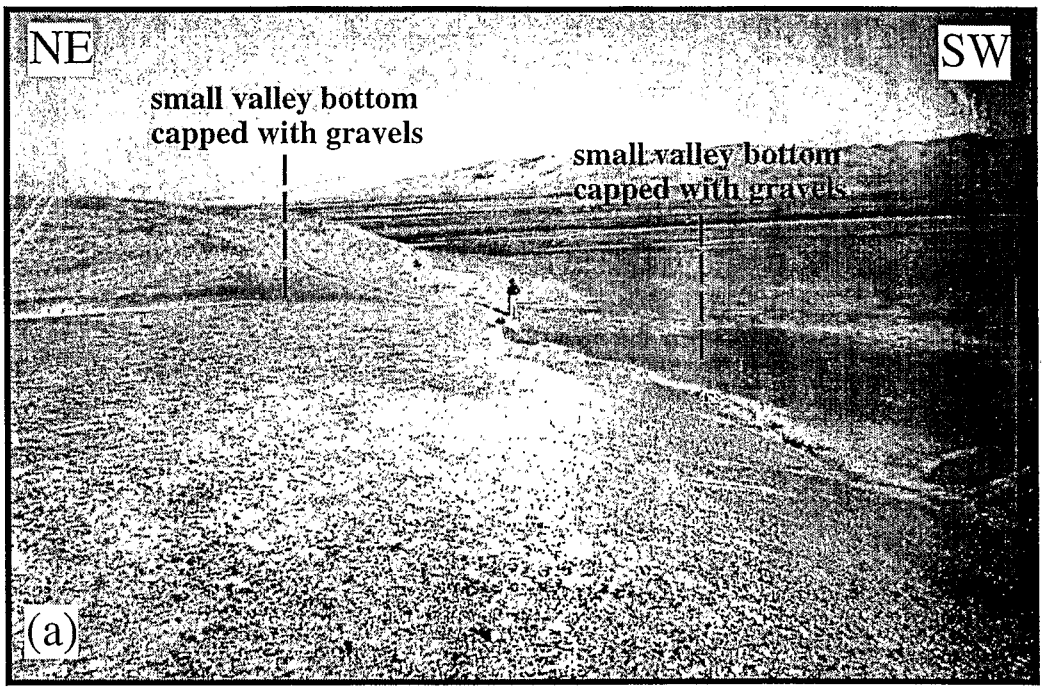

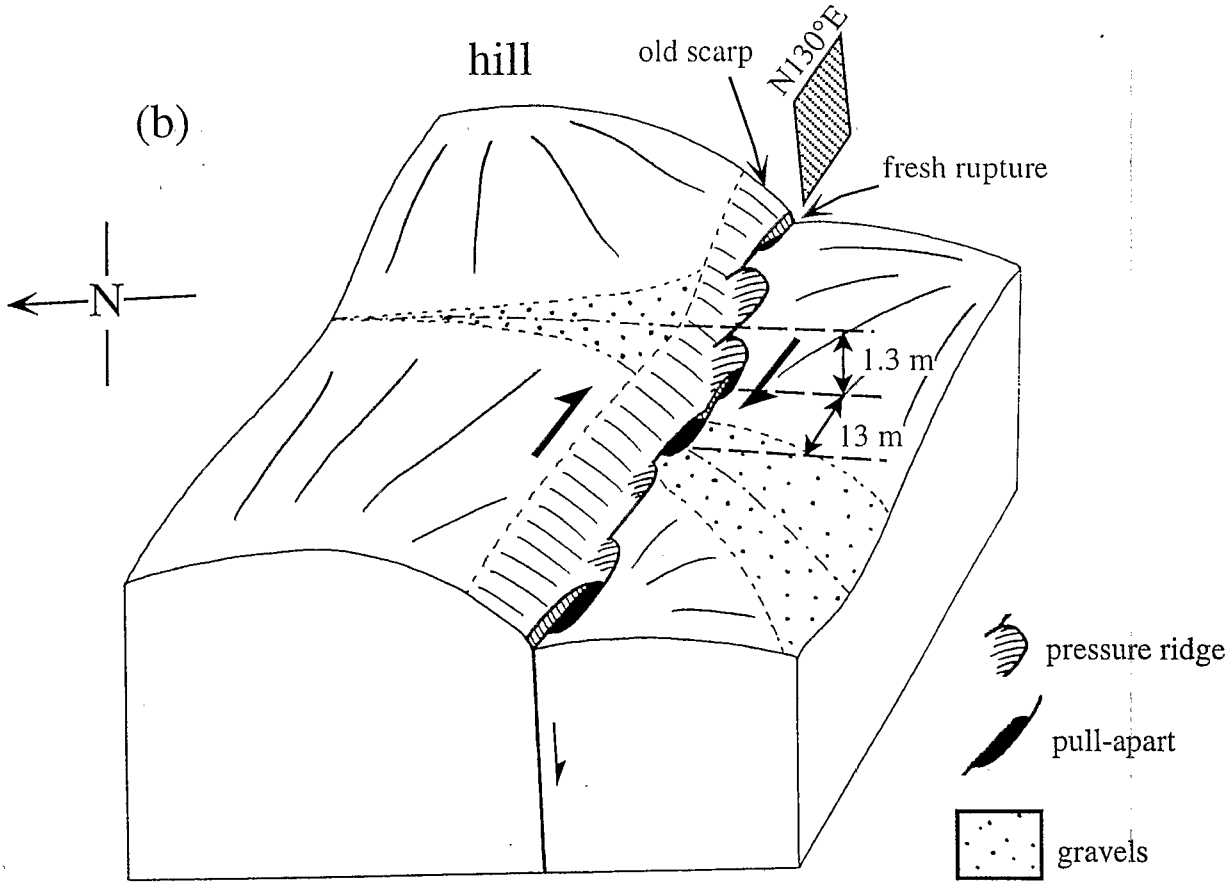

Figure 20. (a) Photograph of the Navidad Fault 2 km NW of Fig. 19. A fresh rupture runs along the foot of an old eroded scarp. The recent rupture exhibits a small vertical (normal) component of displacement of the order of 30 cm but the main component is right-lateral strike-slip as indicated by pressure ridges and pull-apart depressions observed all along the rupture. Depressions along the fault are often unfilled by sediments. A small valley bottom, capped with gravels, exhibits a cumulative offset of 13 m right-laterally and 1.3 m vertically. (b) Block diagram showing the main features of the fault at the same site as (a), but with a different perspective.

Table 1. Neotectonic data incorporated in the stress tensor analysis.

Name	Fault	Lat. (s)	Long. (w)	Strike/dip/rake
F1 (site 6, Fig. 13)	Salar del Carmen fault (La Negra)	23°48.5′	70°19.8′	350/60/–90
F2 (site 1, Fig. 3)	Cerro Fortuna fault	22°45.6′	70°10.5′	005/60/–90
F3 (near site 2)	Cerro Fortuna fault	23°08.5′	70°15.2′	010/60/–90
F4 (site 2, Fig. 4)	Cerro Fortuna fault	23°09.3′	70°15.2′	015/60/–90
F5 (near site 3)	Cerro Fortuna fault	23°26.2′	70°19.2′	015/60/–90
F6 (site 5, Fig. 10)	Salar del Carmen fault	23°26.9′	70°13.5′	020/60/–90
F7 (site 5)	Salar del Carmen fault	23°32.4′	70°15.4′	025/60/–90
F8 (site 9, Fig. 16)	Cerro Gordo fault	23°17.5′	70°23.1′	023/70/–35
F9 (south of site 7)	Cerro Moreno fault	23°23.0′	70°24.7′	030/80/–11
F10 (site 5, Fig. 11)	Salar del Carmen fault	23°29.0′	70°14.5′	030/70/–47
F11 (site 10)	Barazarte fault	24°06.1′	70°11.7′	155/89/180
F12 (site 11, Fig. 20)	Navidad fault	23°48.3′	70°00.0′	130/80/–174

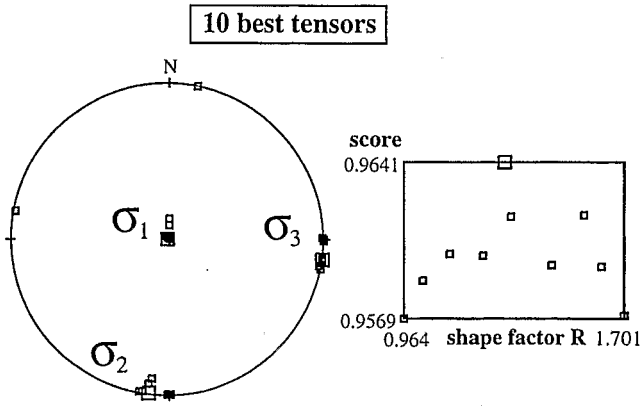

Figure 21. Result of the Monte-Carlo search for the best neotectonic stress tensors for the coastal area in the Antofagasta region. The 10 best tensors are presented in lower-hemisphere equal-area projection. Values of the shape factor R (see text) are plotted with their respective score. The score is the normalized sum of the scalar products between theoretical and observed slip vectors.

suggests a steady uplift during the Quaternary, more consistent with a deep-seated mechanism than with episodic tectonic movements. Average uplift rates are much larger north of the Mejillones Peninsula than south of it. This N–S differentiation in uplift rates is consistent with the general tilt of the planation surfaces on the western Mejillones highland from north to south (Okada 1971). Martinez & Niemeyer (1982) reported that the Caleta Coloso Fault has been inactive during the Quaternary, at least near Caleta Coloso, since it has not displaced the upper Pliocene marine terraces where the fault intersects the coast.

The coastal cliff and offshore morphology

A major cliff, commonly more than 1000 m high and facing west, runs for several hundred kilometres along the eastern margin of the Coastal Cordillera of northern Chile. The continuity of the coastal cliff is interrupted around 23.3°S by the Mejillones Peninsula (Fig. 2). Armijo & Thiele (1990) related the coastal cliff to a major west-dipping normal fault, at present located offshore. Hartley & Jolley (1995) interpreted the coastal cliff as a weathered palaeocliffline which originated through uplift of the coastal margin during Miocene–Pliocene times and inferred that it is not a major extensional fault. They

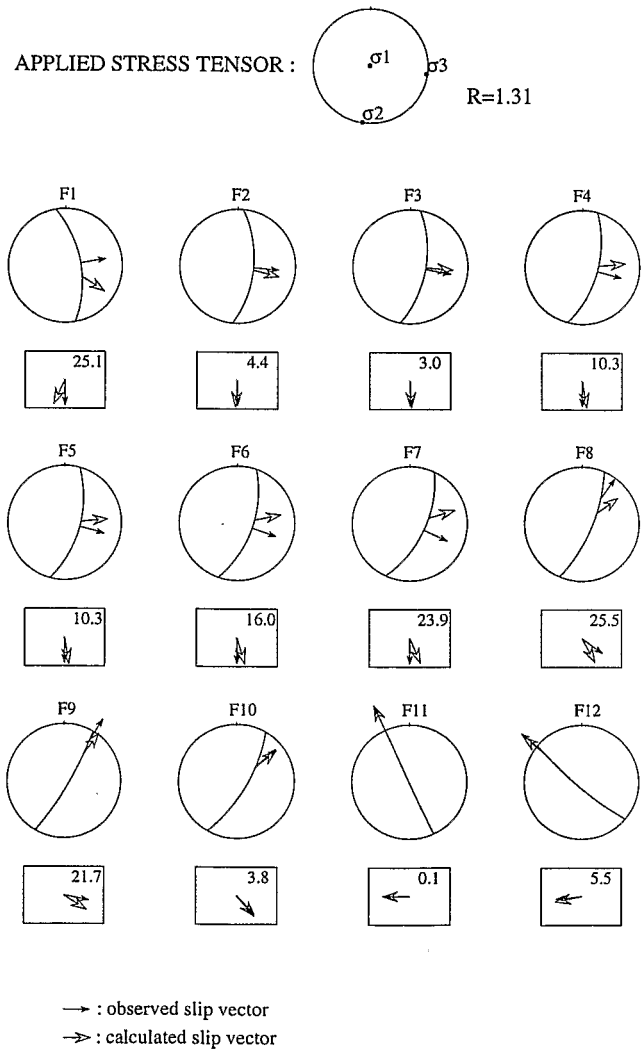

Figure 22. Comparison between theoretical (calculated) and observed slip vectors in stereographic lower-hemisphere projection (circles) and in plane view (rectangles) for 12 neotectonic data incorporated in the stress tensor analysis. Data are listed in Table 1 and the stress tensor applied is the best tensor of Fig. 21. Angular discrepancies between theoretical and observed slip vectors are indicated in degrees on the upper-right corner of the rectangular planes.

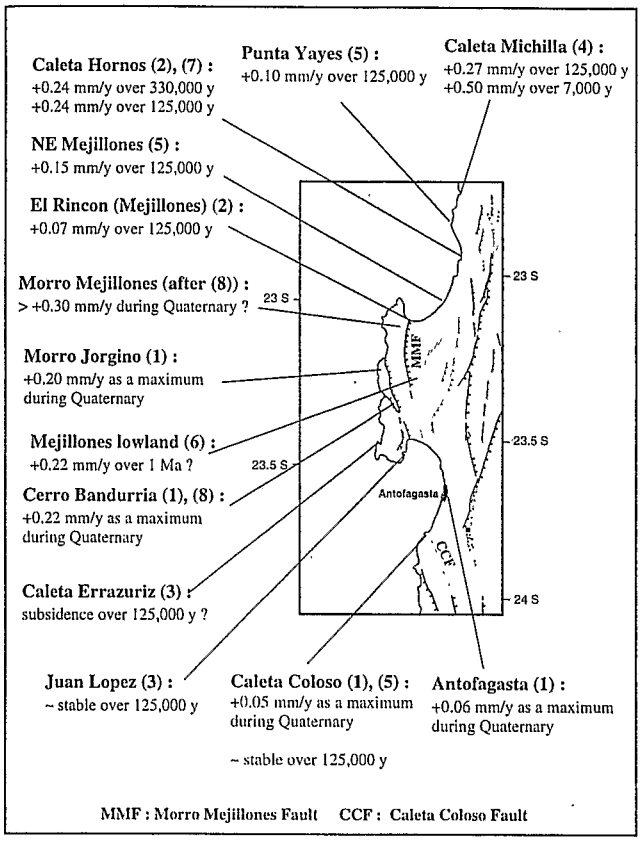

Figure 23. Uplift rates calculated from the height of dated marine terraces. For terraces corresponding to the last interglacial, heights have been corrected for the eustatic, +6 m above present, sea level. Rates are either taken from or calculated from the data given by: (1) Martinez & Niemeyer (1982); (2) Radtke (1987); (3) Ratusny & Radtke (1988); (4) Leonard & Wehmiller (1991); (5) Ortlieb *et al.* (1993); (6) Ortlieb (1993); (7) Ortlieb *et al.* (1994); (8) Ortlieb *et al.* (1996). In the case of the Morro Mejillones, a lower bound for uplift during the Quaternary is given by the present authors, after data in Ortlieb *et al.* (1996). In other places, maximum bounding values of uplift during the Quaternary were calculated from the height of terraces where upper Pliocene marine fauna were found, assuming a 2 Myr age.

noted the absence of any exposed fault breaks along the coastal cliff on aerial photographs and in the field. Wave-cut outcrops of crystalline or volcanic basement are observed in many places in the littoral platform at the foot of the cliff. If the coastal cliff were a major active normal fault scarp, one would expect to find a subsident basin in the hanging wall of the fault, filled with erosional sediments, with its maximum thickness at the foot of the scarp. The basement outcrops indicate that such a basin does not exist. Therefore, if the coastal cliff originated by normal faulting, then it should have retreated considerably (by several kilometres), and the fault should be located offshore, as proposed by Armijo & Thiele (1990).

Fig. 24 shows disruptions in the steep continental-slope topography that may correspond to offshore west-facing normal faults. The outer shelf on both profiles presented in Fig. 24 seems to correspond to a horst block. The horst structure may be a continuous feature between the peninsula and Antofagasta Bay. Bathymetric profiles suggest the existence of a large west-dipping normal fault bounding the outer continental shelf. However, bathymetric and single-channel reflection profiles in Antofagasta Bay (Arabasz 1971) do not show evidence of large vertical offsets associated with an offshore west-dipping fault within 20–30 km from the coast. It is unlikely that the outer-shelf bounding fault generated the coastal cliff 30 km to the east or played a significant role in the Coastal Cordillera uplift. Normal faults dipping towards the trench in the leading edge of the continental plate may simply accommodate the collapse of the margin in response to the general flexure of the margin possibly related to subduction erosion (see below).

Modelling of topography related to faulting

Normal faulting in the Antofagasta coastal area is attested also by a number of 'half-graben' structures with a characteristic width of one or two tens of kilometres. The most spectacular examples are associated with the Atacama, Quebrada Ordonez, Cerro Fortuna and Morro Mejillones faults (Fig. 2). A sequence of three half-grabens can be seen along an east–west transverse around latitude 23°S, as shown in Fig. 2 and more precisely in three dimensions in Fig. 25. Geomorphology and topography appear to be closely related to the main faults, with ranges and basins associated with faulted and tilted blocks. In order to investigate the extent of this relationship, we undertook modelling of topography using a simple model consisting of faults, represented by uniform dislocations, embedded in a homogeneous elastic half-space (Mansinha & Smylie 1971; Savage 1980). Such a dislocation model is valid within the linear elastic theory and is convenient to model small deformation, such as that produced by a single earthquake (coseismic deformation). To model larger deformation produced by repeated faulting we proceed as follows. Deformation is initially calculated at the nodes of a planar regular grid at the surface. Then, step by step, the incremental deformation produced by small fractions of the total displacement on the faults is added to the nodes and the grid deforms non-linearly, giving rise to the topography. The application of step-by-step linear elasticity in this approach produces a calculated topography quite similar to the observed topography. The 3-D problem is considered and nodes at the surface are displaced both vertically and horizontally in response to fault motions. Faults mapped in the rectangular box in Fig. 2 have been digitized and divided into linear segments. In the model, faults have a constant dip of 60° from the surface down to 10 km depth, except the Atacama Fault (Salar del Carmen segment), to which a steeper dip (80°) has been assigned. The choice of the 10 km depth lower boundary for the faults and the unrealistic accumulation of elastic strain around that depth resulting from fault displacements have no significant effects on the surface topography. We postulate that the direction of movement on the fault planes is directly determined by a regional tectonic stress tensor. We used a stress tensor with σ_1 vertical, σ_3 oriented east–west and a shape factor $R=1.5$ (triaxial extension), in agreement with the present neotectonic study (Fig. 21). The amplitude of displacement on the faults has been determined by a trial-and-error procedure. Maximum displacements on the main faults are 1700 m on the Cerro Fortuna Fault, 600 m on the Quebrada Ordonez Fault and 200 m on the Atacama Fault (Salar del Carmen segment).

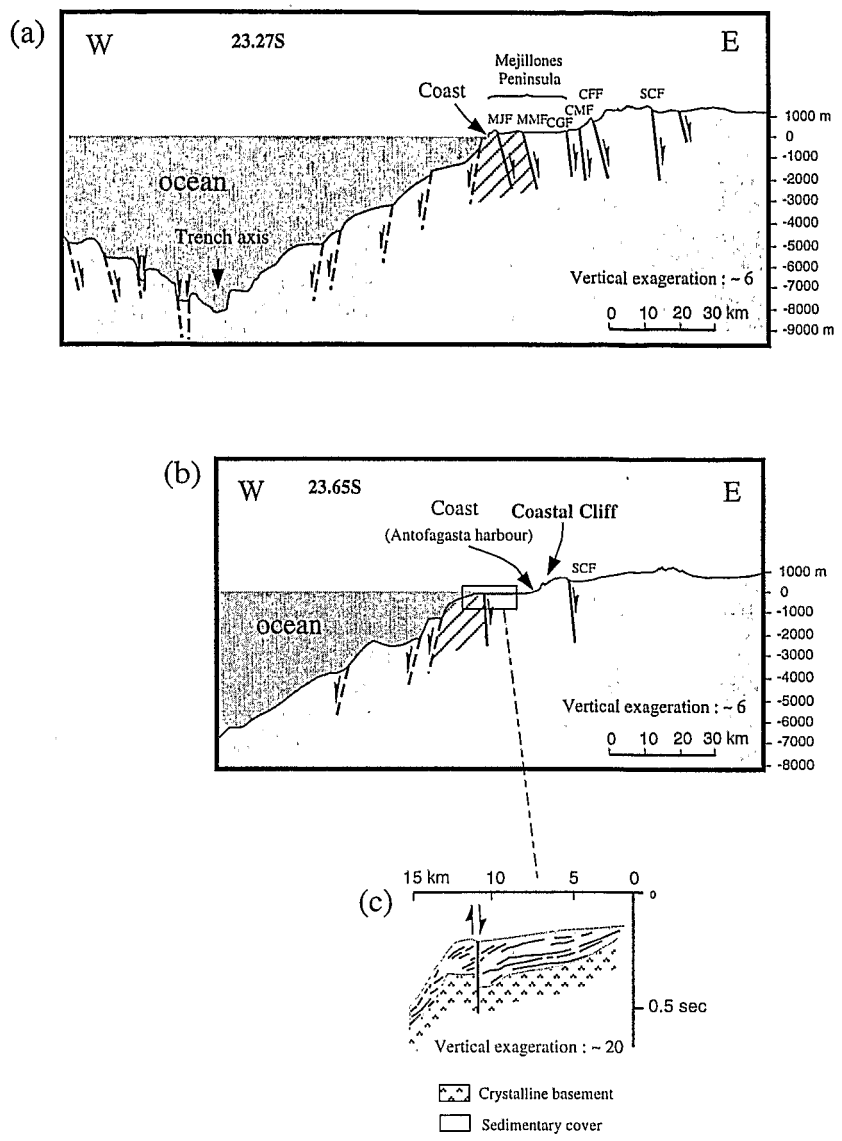

Figure 24. Topographic–bathymetric profiles (a) running through the central part of the Mejillones Peninsula, and (b) through Antofagasta city. Topographic profiles were drawn from 1 : 50 000 maps of the Instituto Geografico Militar de Chile. Bathymetric profile at 23.27°S is from Schweller, Kulm & Prince (1981), and that at 23.65°S is from Arabasz (1971). Profiles are oriented E–W, except the bathymetric part of the southern profile (23.65°S), which is trending N72°E. The hatched areas in (a) and (b) are outer-shelf fault-bounded blocks of horst type. MJF: Morro Jorgino fault; MMF: Morro Mejillones fault; CGF: Cerro Gordo fault; CMF: Cerro Moreno fault; CFF: Cerro Fortuna fault; SCF: Salar del Carmen Fault. (c) Single-channel reflection profile in Antofagasta Bay, redrawn from Arabasz (1971).

Although many aspects of the tectonic processes are neglected in this simple model, such as isostasy, erosion, sediment filling and viscous relaxation of stresses at depth, the actual topography can be reasonably well fitted, provided a regional topographic trend is added to the topographic effect of the faults. The modelled topography is presented in Fig. 26. To approximate the presence of sediment filling in the depressions formed in the hanging wall of the faults graphically, grey-shaded surfaces hiding the depressions have been added to the calculated topography in accordance with the extent of Neogene–Quaternary basins. The agreement between the real and calculated topography can be appraised in two dimensions in the four cross-sections presented in Fig. 27. The regional trend is also shown. The coastal cliff is not reproduced by the model because we do not consider it as a fault scarp. Topography west of the coastal cliff has been hidden in Fig. 26, assuming that marine erosion removed the corresponding material. The general morphology of the westernmost range between the Cerro Fortuna Fault and the coastal cliff is well reproduced without incorporating a west-dipping fault. A somewhat large misfit can be observed in the western part of profile P4 (Fig. 27). An important part of this misfit may be attributed to high fluvial erosion related to large drainage channels (Mejillones and Mittitus Quebradas). Our simple model is not unique but shows how the characteristic short-wavelength (10–20 km long) features of topography in the area can be controlled by the known large faults, under E–W extension.

The E–W extensional stress regime (Fig. 21) was found using observations of young metric-scale offsets. The permanency of this tectonic regime over a much longer period of time is

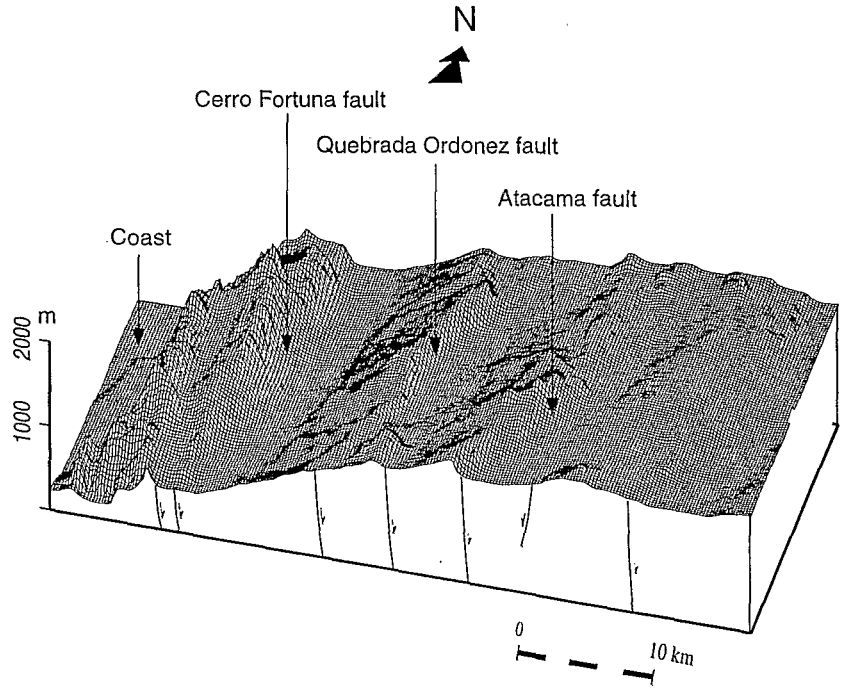

Figure 25. 3-D topography of the coastal area northeast of Antofagasta, around 23°S (see Fig. 2 for location). Scarps of the main faults are indicated, and faults mapped on the southern margin of the area are drawn in cross-section. Topography was digitized from 1:50000 maps of the Instituto Geografico Militar de Chile.

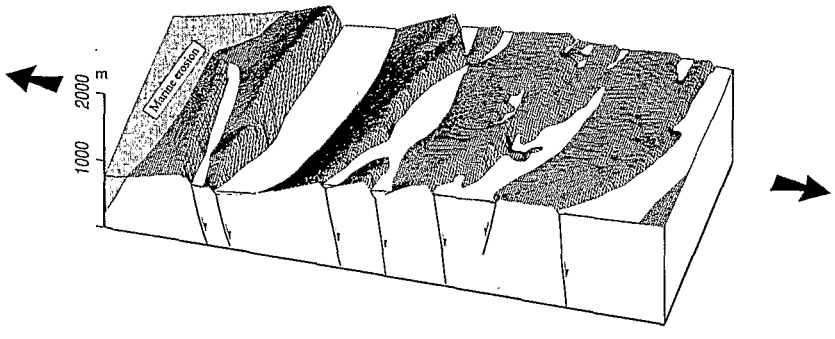

Figure 26. Modelled 3-D topography of the coastal area northeast of Antofagasta, around 23°S (same area as Fig. 25). Light shading represents sediment filling. The dark shaded zone labelled marine erosion represents the removal of material by marine erosion and the formation of the coastal cliff. The arrows indicate the direction of tectonic extension. For details about the modelling process, see text.

strongly supported by modelling the topography. Modelling of the offshore bathymetry was not attempted because the existence of west-dipping faults offshore associated with large vertical offsets (Fig. 24) is not strictly proven in the absence of a high-resolution bathymetric map and seismic profiles.

Regional uplift of the Coastal Cordillera

Armijo & Thiele (1990) reported that the flat erosion surface topping the basement rocks of the Coastal Cordillera, locally covered by 21 Ma ignimbrites, belongs to the regional pediplain formed during the Palaeogene (Coastal Tarapaca Pediplain: Mortimer & Saric 1975; Paskoff 1980; Paskoff & Naranjo 1983). This surface lies at a present elevation of 1000–1500 m in the area of study. Vertical movements related to faulting along the coastal range faults were superimposed on this regional uplift (see preceding section). It has been stated (Paskoff & Naranjo 1983) that during the Miocene the Coastal Cordillera acted as a barrier to erosional and volcanic material coming from the Andes, which then accumulated in the Pampa del Tamarugal (Central Depression). Relative uplift of the coastal range with respect to the Pampa del Tamarugal is therefore younger than 21 Ma and may be partially linked to the initiation of vertical fault motion along the AFS, in agreement with the 19 Ma lower limit for normal-fault activation given by Hervé (1987b). A new planation surface formed before 9 Ma. Pliocene rivers from the high cordillera then started to incise the newly formed surface and developed narrow valleys with depths up to 1000 m (Paskoff & Naranjo 1983). Climatic change may have played some role in the initiation of channel incision (Mortimer 1980; Paskoff & Naranjo 1983). Mortimer (1980) proposed that tectonic steepening of the regional slope of the Andean flank throughout the Neogene may have produced a critical slope favouring channel development. Therefore, part of the 1000 m of uplift

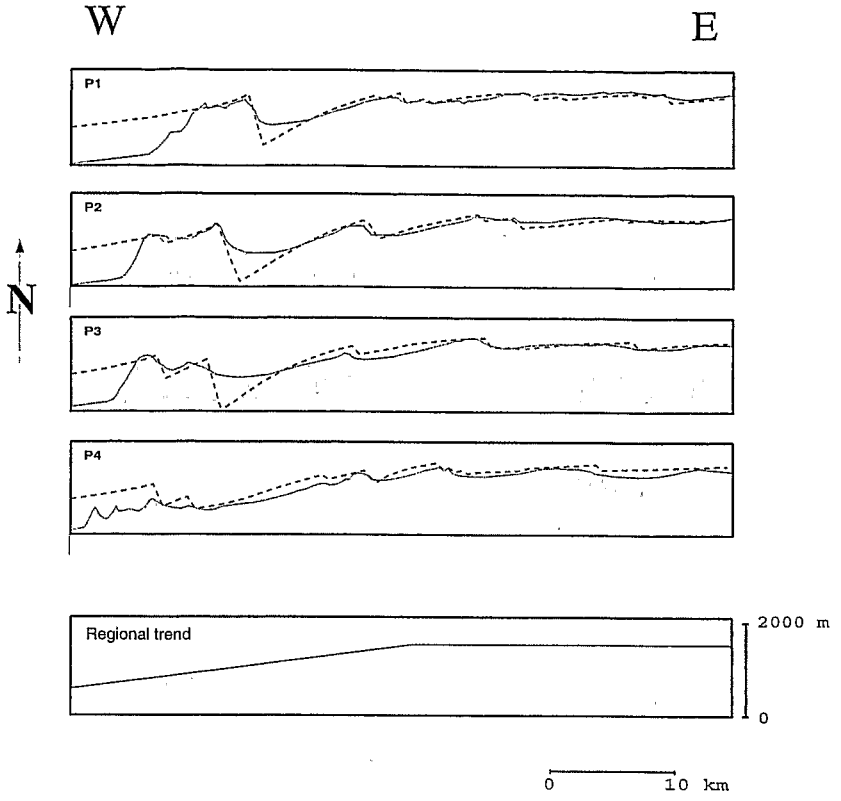

Figure 27. P1 to P4 are four E–W sections across the modelled area. P1 is located in the northernmost part, P4 is in the southernmost part, and P2 and P3 are in the central part of the modelled area. Topography digitized from 1:50 000 maps is represented by the shaded surfaces bounded by continuous lines, whilst the modelled topography is drawn with dashed lines. The regional trend used is shown at the bottom.

of the Pampa del Tamarugal deduced from the depth of Pliocene valleys may have taken place before the Pliocene, that is during the Miocene. Assuming a constant uplift rate from Miocene to present and assuming that the erosion surface topping the Coastal Cordillera was not far from sea level at 21 Ma, long-term uplift rates of 0.05–0.07 mm yr^{-1} are found (1000–1500 m in 21 Myr). Uplift rates in the Central Depression (Pampa del Tamarugal) are more difficult to estimate because the initial elevation of the Neogene pediplain is not known. Armijo & Thiele (1990)'s hypothesis of 1000 m of uplift since the late Miocene ($\approx$9 Ma) would indicate a rate of 0.11 mm yr^{-1}, but a distributed uplift since the early Miocene would give a rate similar to that of the Coastal Cordillera. Similar uplift rates of 0.06–0.10 mm yr^{-1} from the early Miocene to the present have been documented for the Coastal Cordillera in southernmost Peru, suggesting that the continental margin of the Central Andes has, on a broad scale, responded uniformly to plate subduction since the early Miocene (Tosdal, Clark & Farrar 1984). Constraints on Quaternary uplift on the western margin of the Coastal Cordillera are given by the heights of marine terraces (Fig. 23). Upper Pliocene marine terraces are located at only about 100 m above sea level near Antofagasta (Martinez & Niemeyer 1982), indicating Quaternary uplift rates of 0.05–0.06 mm yr^{-1} (Fig. 23), in agreement with the longer-term estimates given above. On the other hand, uplift rates two to four times larger than the longer-term average are found for the late Quaternary along the coast north of the Mejillones Peninsula (Fig. 23).

INTERACTION BETWEEN THE SUBDUCTION PROCESS AND FOREARC TECTONICS

Short-term interaction: the subduction earthquake cycle

By short-term interaction we mean processes of interaction varying rapidly, at a scale of years or decades. Short-term interaction essentially involves the mechanisms operating during the subduction seismic cycle.

The effect of the coseismic phase on surface deformation, corresponding to the occurrence of a large subduction earthquake along the shallow part of the plate interface, is well modelled by dislocations in an elastic medium [see e.g. Plafker & Savage (1970) and Barrientos & Ward (1990) for the great 1960 Chile earthquake, and Fitch & Scholz (1971) for the 1946 Nankaido, Japan, earthquake].

The largest subduction earthquake which occurred this century in northern Chile is the M_w=8.0 Antofagasta earthquake of 1995 July 30. This earthquake was studied in detail by Ruegg *et al.* (1996) and by Delouis *et al.* (1997). Coseismic deformation has been modelled and implications for the continental tectonics are discussed in the present paper.

Surface deformation related to the M_w=8.0 Antofagasta earthquake of 1995 July 30

This large subduction earthquake occurred near Antofagasta, three months after our neotectonic field survey. Data from a

local network installed previously in the region, together with waveform modelling of teleseismic broad-band records, permitted the detailed modelling of the rupture process of the earthquake (Delouis *et al.* 1997). The main rupture started underneath the southern margin of the Mejillones Peninsula and propagated southwards over an area of 185 km × 90 km with a velocity of 2.8 km s^{-1}, in a N200° direction. Most of the seismic moment (80 per cent) was released in the first 120 km of rupture. The main rupture corresponds to a thrust along the subduction interface between 10 and 50 km in depth.

The source parameters obtained from broad-band waveform modelling were used to estimate the surface displacement and stress changes generated by the main shock. This was done using the method of Mansinha & Smylie (1971), and by superposition of several dislocations within an elastic half-space simulating the rupture (Savage 1980). Fig. 28 shows the horizontal projection of the elements into which the rupture surface was divided and their associated dislocations. The calculated vertical displacements fit within a few centimetres the observed values of coastal uplift (Fig. 28b). The maximum values for the calculated horizontal displacement onshore are 100 cm towards the WSW. These values are observed along the coast above the central part of the rupture (Fig. 28c) and fit within a few centimetres the absolute values of displacement derived from GPS measurements made before and after the

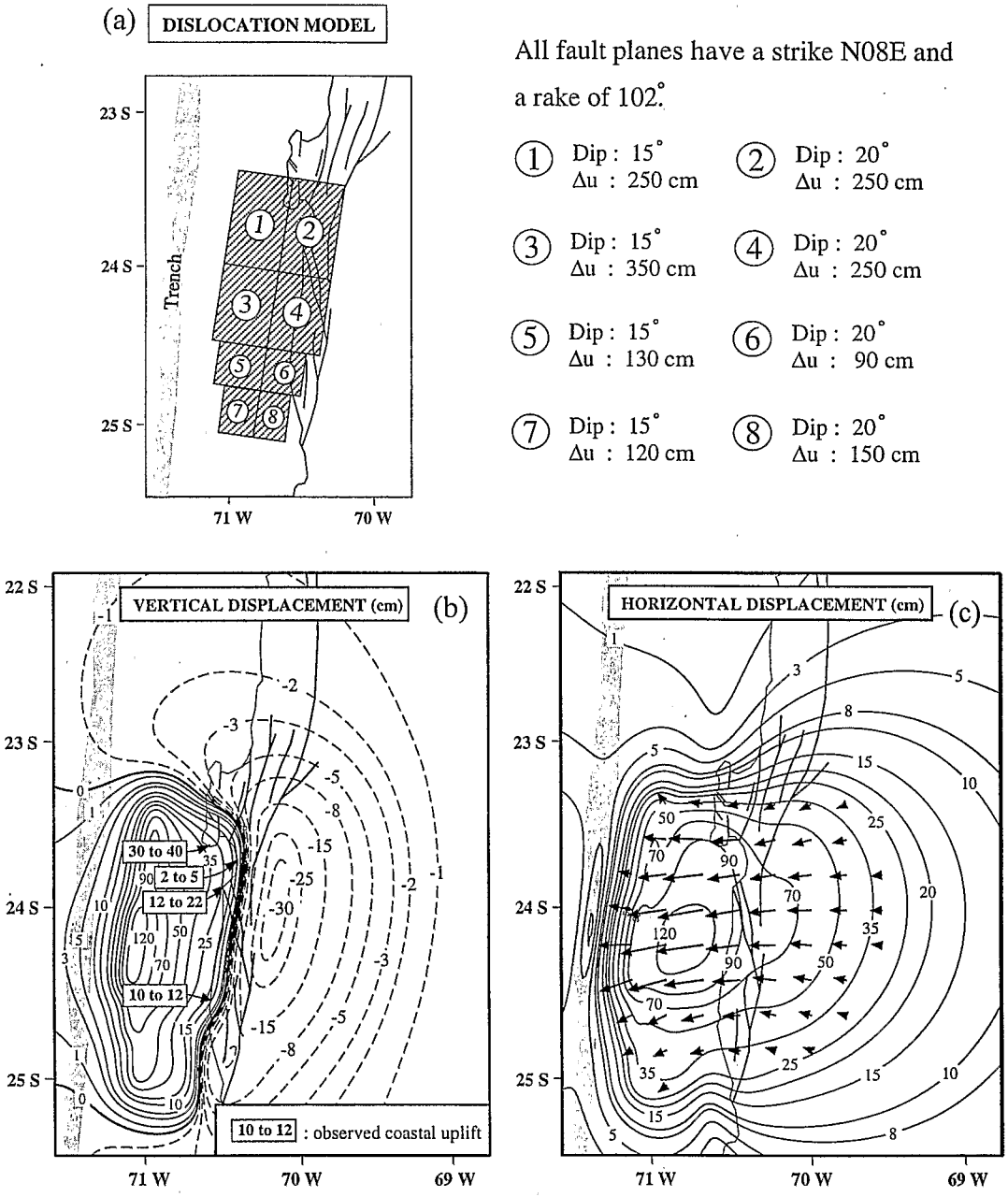

Figure 28. (a) Dislocation surfaces simulating the rupture of the 1995 Antofagasta earthquake, obtained from waveform modelling and from the geometry of aftershock distribution (Delouis *et al.* 1997). (b) Vertical, and (c) horizontal static displacements at the surface calculated from the source model shown in (a). Values of observed coastal uplift in (b) are from Ortlieb *et al.* (1995).

earthquake (Ruegg *et al.* 1996). Both the calculated displacements (Fig. 28c) and GPS measurements show that the WSW motion increased from east to west in the Coastal Cordillera, implying E–W extension. Although the main rupture occurred 30–50 km below the onshore area, the 1995 July 30 earthquake activated the Atacama Fault System slightly, in particular along the Paposo fault segment. Fig. 29 shows a fresh break several hundred metres long, photographed in August 1995, cutting into the alluvial fans some 20 m downslope of the main fault trace (site 12, Fig. 2). We did not observe this rupture in April 1995, though we closely examined the same fault segment. For this reason we associate this rupture with the 1995 Antofagasta earthquake. The rupture was observed during the aftershocks recording campaign, although we could not map precisely the breaks over the total length of the rupture. Fig. 30 shows detailed views of the scarp where a normal vertical offset of some 15–20 cm is seen. No clear indication of lateral offset was found. These breaks cut across several alluvial fans and are therefore tectonic and not due to gravitational sliding or compaction; moreover, some are observed along the fault trace in places where the surface topography is flat. It has been mentioned that the Paposo segment is suspected to be inactive at present. Therefore, it must be recognized that faults may be slightly reactivated after a long period of inactivity. We propose a similar context for the recent rupture observed at the northern extremity of the Cerro Fortuna Fault (site 1).

The Paposo fault segment is located above the eastern border of the main rupture of the 1995 July 30 earthquake. Fig. 31 shows how the stress change induced by the main rupture favours normal faulting in the area where surface ruptures have been observed. We calculated the stress change at 3 km depth inside the continental crust because a significant rupture could not nucleate at the surface. The earthquake produced horizontal extension perpendicular to the Atacama Fault. More precisely, the focal mechanism in Fig. 31 indicates the hypothesized faulting that the 1995 July 30 earthquake would have induced on the Atacama Fault if it had the ability to activate the fault in the absence of previously accumulated stresses. It has been assumed that the fault is dipping 75° towards the east and that the slip vector has the same direction and sense as the applied shear stress (Bott 1959). This hypothetical focal mechanism is compatible with the normal fault breaks observed at the surface (Fig. 30).

We also calculated the Coulomb stress change induced by the Antofagasta earthquake. The Coulomb stress change (CSC) has been used in a number of studies to investigate the triggering effect of earthquakes on nearby faults (see e.g. King, Stein & Lin 1994). We used the following definition: $CSC = \Delta\tau - \mu\Delta\sigma_n$, where $\Delta\tau$ is the shear stress change on the fault plane, $\Delta\sigma_n$ is the normal stress change (positive for compression) on the fault plane and μ is the coefficient of friction. The value $\mu = 0.6$ has been used, and changes in fluid pressure were neglected. The Coulomb stress change induced by the 1995 July 30 earthquake is calculated at 3 km depth for a fault plane striking N05°E and dipping 75° towards the east. Values of CSC are positive, indicating the potential for triggering (Fig. 31). At the site where new surface ruptures have been observed, $CSC = +2.8$ bar. It has been stated that stress changes of the order of a few bars or less can trigger seismicity on pre-existing faults (Simpson 1986). King *et al.* (1994) showed how the $M = 6.5$ Big Bear earthquake was apparently initiated by a Coulomb stress change of 2–3 bar as a result of the $M = 7.4$ Landers earthquake. Static stress drops of most

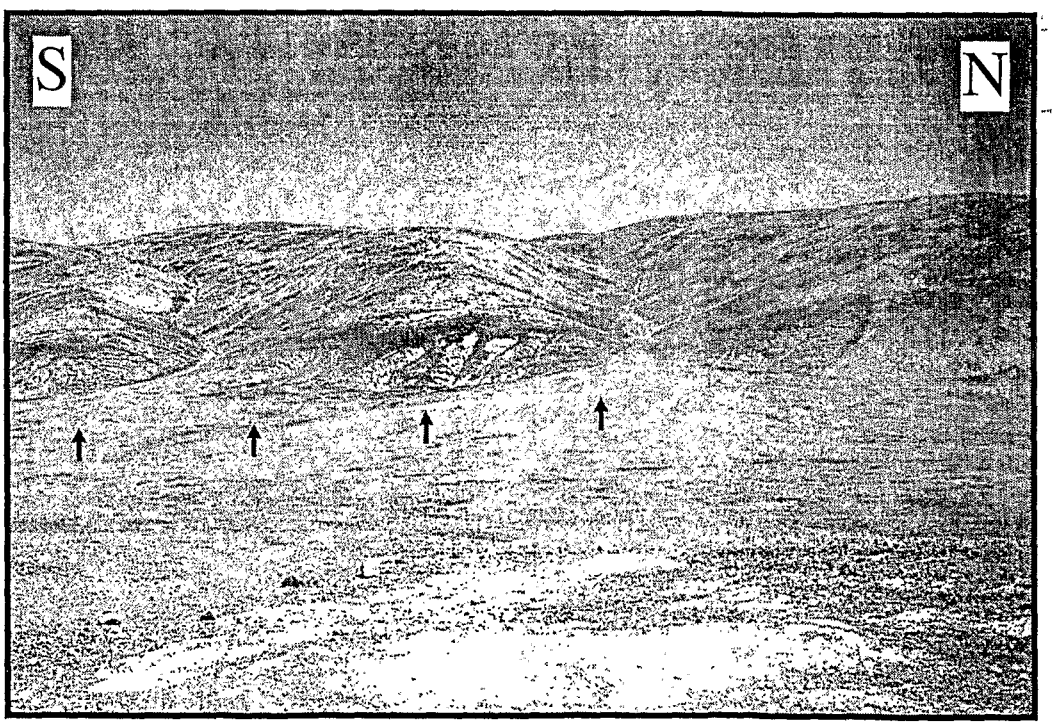

Figure 29. New fresh scarp several hundred metres long along the Paposo fault segment (Atacama Fault, see Fig. 2, site S12, for location). This scarp was not present in April 1995 and it was photographed three weeks after the Antofagasta earthquake of 1995 July 30. Although the 1995 July 30 earthquake occurred along the subduction interface, it generated horizontal extension in the upper crust and triggered faulting along the Atacama Fault.

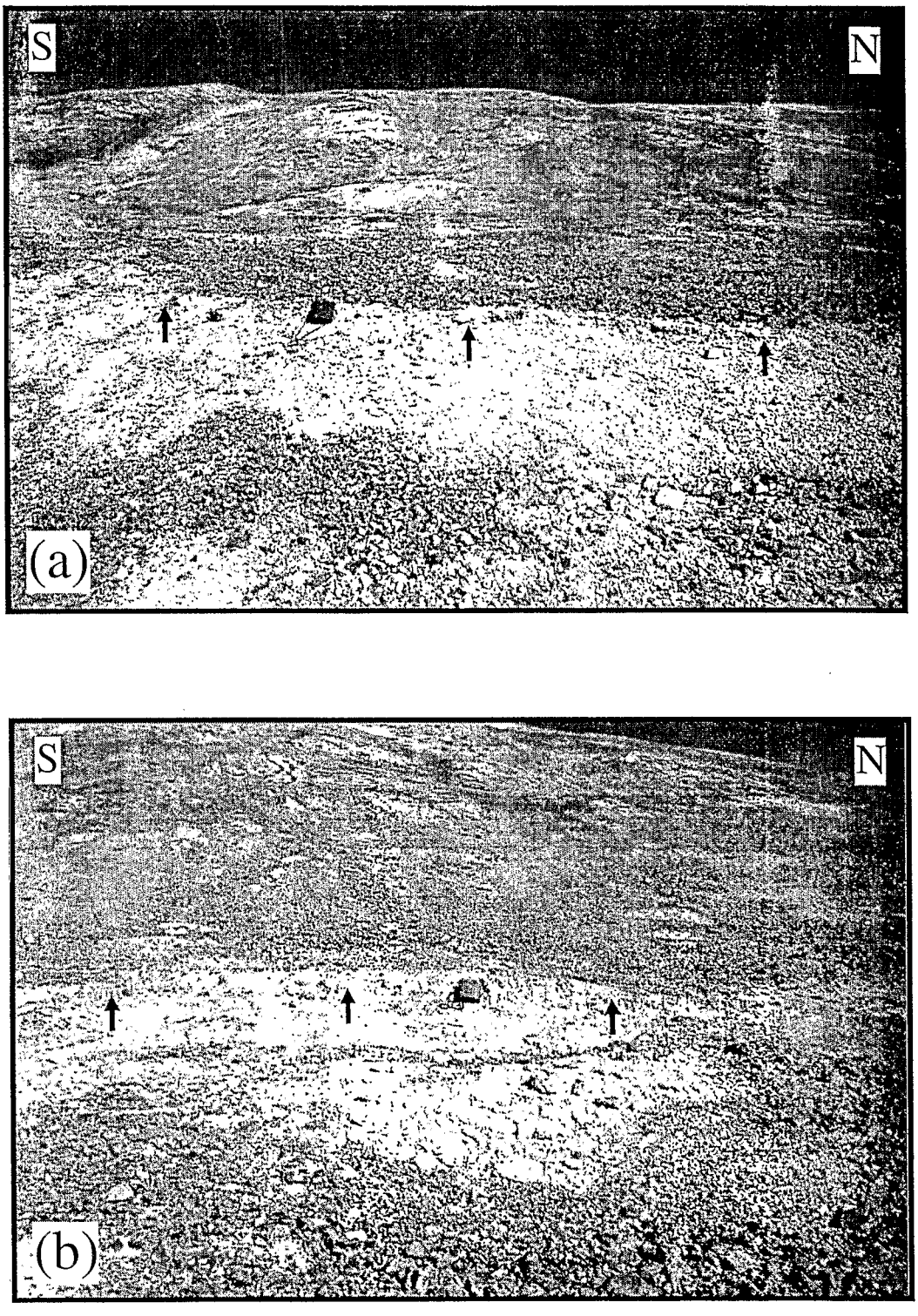

Figure 30. (a) and (b) Two photographs showing details of the new fresh scarp along the Paposo fault segment (same rupture as that shown in Fig. 29). A normal fault offset of 15–20 cm is observed. An 18 cm high binoculars case is shown as reference. Arrows outline the base of the scarp. The offset alluvium, made up of clasts veneered with a dark desert varnish, appears very old, implying a very low slip rate/very long recurrence in time.

large ($M > 5.5$) earthquakes are in the range 10–100 bar (Kanamori & Anderson 1975). The calculated 2.8 bar Coulomb stress change is enough to trigger an earthquake on the Atacama Fault, provided that the fault has been previously loaded by at least several bars towards normal faulting.

Coseismic deformation and marine terraces

The pattern of surface deformation produced by the 1995 July 30 earthquake and the deformation deduced from marine terraces are very different. Significant coseismic uplift

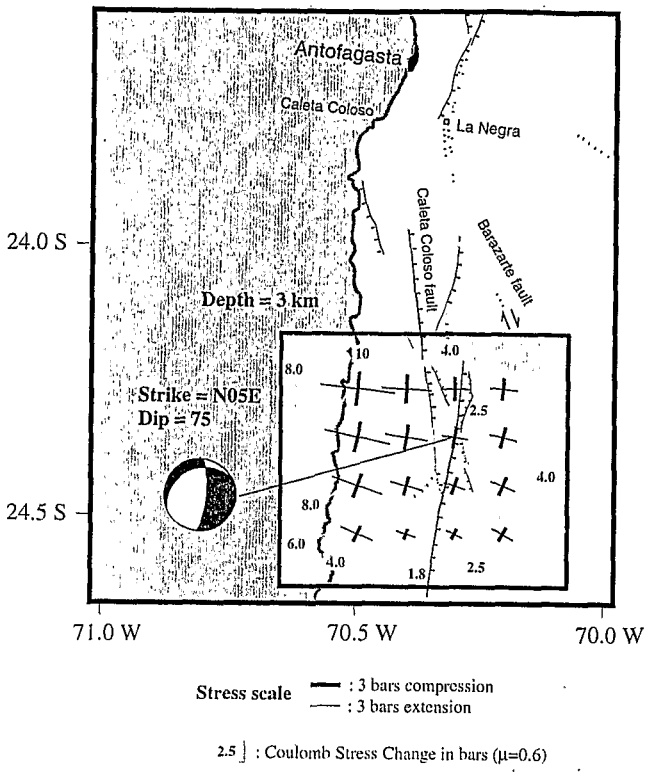

Figure 31. Horizontal deviatoric stresses and Coulomb stress change induced by the 1995 Antofagasta subduction earthquake in the coastal area south of Antofagasta. The area where stresses have been calculated is framed and shaded in light grey. Stresses have been calculated at 3 km depth. The focal mechanism indicates the hypothesized faulting that the 1995 subduction earthquake induced on the Atacama Fault (Paposo fault segment, strike N05°E, dip 75°). The focal mechanism is represented on the lower-hemisphere equal-area projection and has been calculated at the site where new surface ruptures have been observed along the Paposo fault segment.

is observed on the southern margin of the Mejillones Peninsula (30–40 cm) and at Antofagasta–Coloso (12–22 cm) (Fig. 28b), where near stability or slight subsidence has been established for the last 125 000 years (Fig. 23). On the other hand, the earthquake produced coastal subsidence of a few centimetres in the northern part of the Mejillones Peninsula and along the coast further north, a zone which shows the highest long-term uplift rates (Fig. 23). Of course, the occurrence of a large subduction earthquake north of the Mejillones Peninsula will somehow reduce these latter discrepancies. However, the high coseismic uplift at the southern extremity of the Peninsula would certainly not be reduced to zero. Surface deformation related to slow aseismic deformation at depth downdip of the coseismic rupture, taking place in the years or decades following the 1995 July 30 earthquake, together with broad-scale deformation related to plate motions in the interseismic phase, may be the processes by which coastal uplift will come closer to its long-term average after completion of a seismic cycle.

Marine terraces indicate higher upper Pleistocene to Holocene uplift rates in the northern part of the Mejillones Peninsula and further north than to the south. This difference in uplift rate may reflect a difference in the subduction regime. North of 23–24 S interplate coupling is strong and historical data (Comte & Pardo 1991) suggest that large earthquakes of magnitude 8.5–9 occur with a recurrence rate of 100–150 years. On the other hand, in the region between Antofagasta and Paposo (≈23.5°S–25°S), no earthquake of magnitude greater than 8 has been reported since 1800, the time when historical information began.

Long-term interaction: mechanisms for long-lived extension

By long-term interaction we mean mechanisms operating at the subduction zone with properties and effects varying only slowly, at the timescale of several thousands to millions of years.

A change in the dip angle of the plate interface near the trench has been proposed by Mortimer & Saric (1975) as a possible cause for extension in the leading edge of the continent. Armijo & Thiele (1990) proposed that the extension, and the existence of a large west-dipping fault of crustal scale related to the coastal cliff, may be explained by a change in dip at the subduction interface (subduction ramp). An abrupt change in dip (subduction ramp) is not supported by the distribution of aftershocks of the 1995 Antofagasta earthquake (Delouis *et al.* 1997), but the influence of a gradual change in dip of the shallow portion of the slab interface cannot be disregarded.

Hartley & Jolley (1995) considered that regional uplift during the Plio–Pleistocene may have been produced by the subduction of an aseismic ridge centred around the Mejillones Peninsula. However, this ridge is one order of magnitude wider than the Mejillones Peninsula and, furthermore, the information about the subducted part of the ridge is lost.

Subduction erosion (also called tectonic erosion) has been contemplated as the mechanism responsible for outer forearc extension in Japan and Peru (von Huene & Lallemand 1990). On the other hand, underplating of material eroded by subduction beneath parts of the upper plate has been proposed as a mechanism responsible for topographic uplift (von Huene & Lallemand 1990). Although offshore subsidence has not been directly demonstrated in northern Chile, several indirect lines of evidence point towards active subduction erosion and underplating in northern Chile: the migration of the magmatic arc (Rutland 1971; Coira *et al.* 1982; Scheuber & Reutter 1992); higher $^{87}Sr/^{86}Sr$ ratios of mafic magmas erupted in northern Chile in comparison to southern Chile (Stern 1991); the spatial distribution of the Palaeozoic basement and the Jurassic Andean magmatic belt (Stern 1991); the abnormal thickness (40–50 km) of the continental crust in the forearc with regard to the small amount of crustal shortening in the area (Schmitz 1994); high seismic velocities observed at only 20 km depth beneath the Coastal Cordillera, underlain by an anomalous low-velocity zone down to the Moho (Reutter *et al.* 1988; Wigger *et al.* 1994; Schmitz 1994).

Origin of the forearc state of stress

We propose that three mechanisms contribute to the state of stress in the forearc (Fig. 32). Combining those three mechanisms will result in a strongly time-dependent state of stress. Here, we do not discuss the nature and the origin of the forces that drive the plates but consider only a kinematic kind of boundary condition.

(1) The first contribution to the state of stress in the forearc considered here comes from large subduction earthquakes (Fig. 32a). These events correspond to the breaking of the asperities along the shallow plate interface which locally

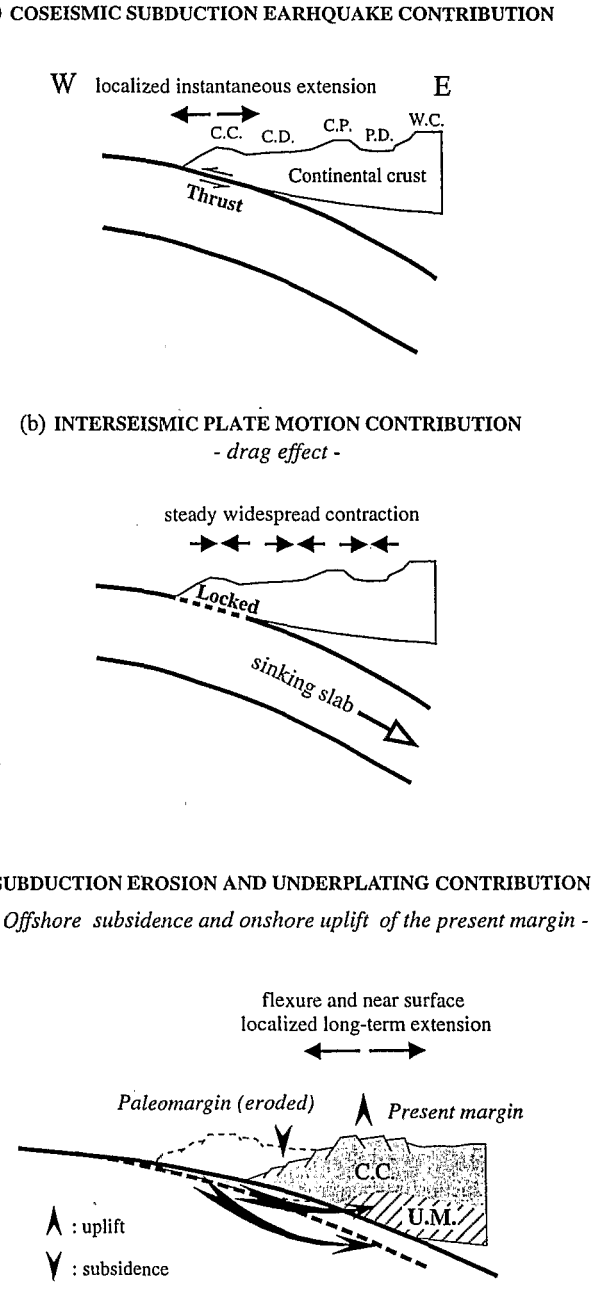

Figure 32. Composite state of stress in the forearc. (a) Contribution of subduction (thrust) earthquakes. (b) Contribution of slow plate motion during the interseismic phase. (c) Contribution of subduction erosion and underplating. C.C.: Coastal Cordillera; C.D.: Central Depression; C.P.: Chilean Precordillera; P.D.: Preandean Depression; W.C.: Western Cordillera; U.M.: underplated material.

hindered or slowed relative motion between the plates. We have shown how the Antofagasta earthquake (M_w=8.0, 1995 July 30) produced extension perpendicular to the trench in the coastal area (Fig. 31). Similar extension has been observed from geodetic data in the case of the 1960 southern Chile earthquake (Plafker & Savage 1970, modelled by Barrientos & Ward 1990) and in the North Island of New Zealand (1931 Hawke's Bay earthquake, Walcott 1978). Horizontal extension in the uppermost crust originates in the gradient of near-surface horizontal trenchward motion. Large gradients of horizontal calculated displacement associated with the Antofagasta earthquake are mainly concentrated above the subduction rupture surface and decrease rapidly further inland (Fig. 28c). A subduction earthquake's contribution to plate motions and to the upper plate deformation is limited to the forearc area and is concentrated in the outer forearc (Coastal Cordillera and offshore area).

(2) The second contribution comes from plate motions in the intervening time between two large subduction earthquakes, corresponding to the interseismic phase (Fig. 32b). During this stage, the plate interface between two plates is locked at shallow depth and the forearc continental region is coupled to the sinking slab. The slab pull force is transmitted to the continental plate (drag effect) which, as a result, is submitted to E–W contraction. Contraction in the direction of convergence has been documented by geodetic data in Japan over a 60 year period in areas where no large subduction earthquake occurred (Mogi 1970), in the Cascadia subduction zone over a 10 year period (Savage, Lisowski & Prescott 1991) and in the Northern Island of New Zealand before the 1931 M=7.9 Hawke's Bay earthquake (Walcott 1978). In this interseismic phase, compressional stresses rise gradually with time as plate motions proceed. Finite-element modelling of Andean-like subduction zones (Bott, Waghorn & Whittaker 1989; Whittaker, Bott & Waghorn 1992) support a broadly distributed contraction of the forearc region due to slab pull when the plate interface is locked.

(3) The third possible contribution comes from subduction erosion (tectonic erosion), along with underplating in the forearc (Fig. 32c). The slope in the forearc wedge is increased by the removal of material at the base of the overriding plate near the trench (Lallemand, Schnürle & Malavielle 1994). Accordingly, normal faulting would accommodate the near-surface deformation of the subsiding (downdropping) wedge. Extension both along the continental slope and in the near-shore coastal range may reflect the broad-scale flexure of the outer forearc (see Figs 24 and 25). Such flexure is always present in subduction forearcs but would be considerably accentuated by active subduction erosion and possibly by underplating. von Huene & Lallemand (1990) showed that the present morphology of the Peruvian margin was formed during the last 20 Myr, as indicated by well-documented 4–5 km Neogene subsidence (von Huene & Lallemand 1990; von Huene & Scholl 1991). Since similar rates of tectonic erosion have been estimated for Peru and northern Chile (von Huene & Scholl 1991), flexure of the present margins of Peru and northern Chile is expected to have similar ages. Initiation of vertical motion along the Atacama Fault System similarly occurred in the early Miocene (21–19 Ma), as shown above. Therefore, it may be suggested that subduction erosion and extensional tectonics in the present outer forearc of northern Chile are coeval, and that a causal relationship between the two phenomena exists. The systematic dip towards the east of the faults in the Coastal Cordillera may be explained by counterclockwise rotation of initially near-vertical faults when the flexure was formed.

The state of stress in the outer forearc (Coastal Cordillera and offshore area) will remain in the extensional domain (in a deviatoric sense) in the long-term if the balance between coseismic extension and interseismic contraction is in favour of extension. This means that the net strain produced by a complete seismic cycle is extensional. This occurs, in our

opinion, because coseismic deformation is more concentrated in the outer forearc than interseismic deformation. Subduction erosion and underplating can be viewed as mechanisms which provide a steady component of extension in the outer forearc, in contrast to the seismic cycle contribution, which is strongly time-dependent.

We will now propose an explanation for the coexistence of recent surface ruptures and the absence of small earthquakes in the upper continental crust of northern Chile. We present an argument based on a simple theoretical analysis using the Coulomb failure criterion, which links apparently incompatible observations. The Coulomb stress, defined as $CS=\tau-\mu\sigma_n$, where τ is the shear stress on a fault plane, σ_n is the normal stress (positive for compression) on the fault plane and μ is the coefficient of friction, is always negative, save when failure (slip) occurs ($CS=0$). As a starting point, we assume that a permanent E–W deviatoric extension has been achieved in the outer forearc and that we are in an extensional tectonic regime. We have shown how a large subduction earthquake generates E–W extension in the coastal area consistent with the regional stress tensor determined from neotectonic data and how it produces an increase in Coulomb stress on a crustal fault (positive Coulomb stress change, Fig. 31). On the other hand, it has been established that the intervening time between two large subduction earthquakes is associated with a gradual contraction in the forearcs (see above). Fig. 33 shows how a sequence of seismic cycles along the subduction interface may lead to failure on a specific fault of the Coastal Cordillera. Each subduction earthquake (SE) produces an instantaneous increase in Coulomb stress. Such an increase means an approximation to failure. Next, contraction induces a decrease in Coulomb stress during the time span between two subduction earthquakes, because changes in shear and normal stresses on the fault will be roughly opposite in sense to the shear and normal stresses produced by the subduction earthquake. The condition for crustal normal faulting is that the increase in Coulomb stress in the outer forearc produced by a large subduction earthquake should be larger, on average, than the decrease in Coulomb stress generated in the period separating two subduction earthquakes ($|a|>|b|$ in Fig. 33). This condition has to be fulfilled in order to have a Coulomb stress build-up after each seismic cycle. For the sake of simplicity we assumed a constant rate of Coulomb stress decrease with time in the interseismic phase and we considered only the effects of large earthquakes. A constant rate of contractional strain build-up taking place during several decades has been reported before the 1946 Nankaido earthquake (southwest Japan, Fitch & Scholz 1971). The Coulomb stress on the fault rises over repeated cycles and finally the Coulomb failure criterion will be fulfilled and crustal faulting will occur. This process is consistent with crustal faulting and large subduction earthquakes occurring simultaneously. In the case where crustal faulting was not triggered, the fault will certainly remain aseismic up to the occurrence of the next subduction event (AS, Fig. 33), because a decreasing Coulomb stress means a departure from failure conditions. A large crustal faulting event will produce a strong instantaneous decrease in the Coulomb stress on the fault. It may be followed by aftershocks and, afterwards, the process of Coulomb stress build-up will start again. Of course, the argument may be developed in a more complex form in order to take into account a more realistic situation in which several asperities with different Coulomb failure thresholds are present on the crustal fault plane. In that case, different sizes of crustal earthquakes may be considered. Also, dynamic conditions may modify the argument by increasing the probability of joint subduction and crustal events.

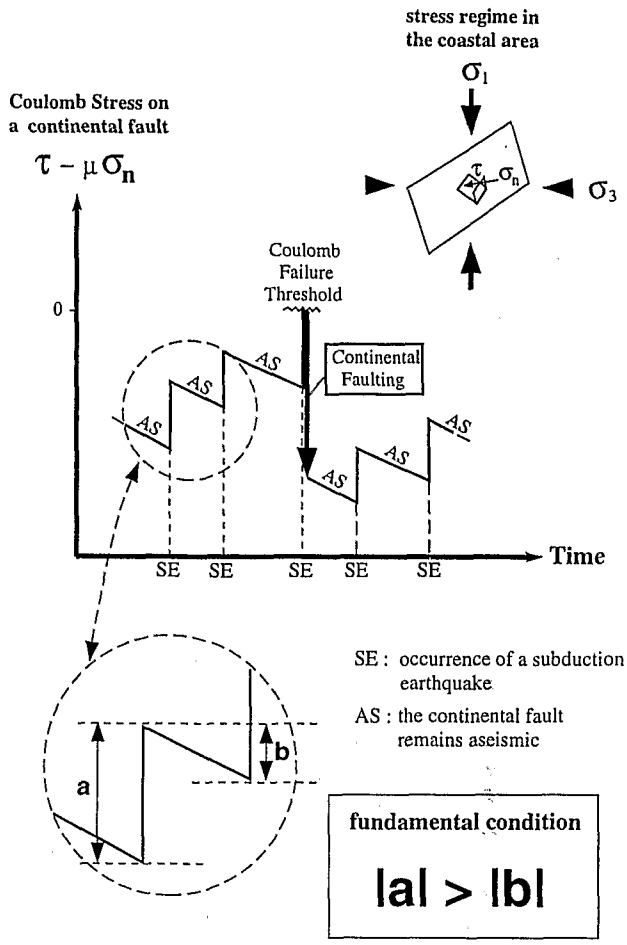

Figure 33. Time evolution of the Coulomb stress on a crustal fault plane of the Coastal Cordillera during the subduction seismic cycle. As a starting point, it is assumed that an extensional stress regime has been achieved in the Coastal Cordillera (σ_1 is vertical and σ_3 horizontal). Subduction earthquakes (SE) are large thrust earthquakes along the shallow part of the subduction plate interface. τ, σ_n and μ are, respectively, the shear and normal stresses and the coefficient of friction on the continental fault plane. Subduction earthquakes generate instantaneous horizontal extension which produces an increase in Coulomb stress (a) on the continental fault. On the other hand, during the interseismic phase of the subduction cycle, the Coulomb stress decreases due to steady contraction (b). If $|a|>|b|$, a positive increase in Coulomb stress will remain after completion of each seismic cycle, and eventually the Coulomb failure criterion ($\tau-\mu\sigma_n=0$) will be fulfilled on the continental fault which will slip. During crustal faulting, the shear stress on the continental fault will drop and the Coulomb stress will decrease instantaneously. The process of gradual Coulomb stress increase over repeated subduction seismic cycles will then start again. In the intervening time between two subduction earthquakes, the continental fault will remain aseismic because a decrease in Coulomb stress means that the fault will be further prevented from slipping.

Furthermore, we did not explicitly take into account the 'post-seismic phase' in the above argument.

The argument presented above has been developed to describe the outer forearc tectonics (offshore margin and Coastal Cordillera). We will comment briefly on the implications for the inner forearc areas, comprising the Central Depression, the Chilean Precordillera and the Preandean Depression (Fig. 1). Stress changes related to large subduction earthquakes decrease rapidly landwards of the downdip extent of the rupture along the plate interface. Even if a larger surface rupture than that of the 1995 Antofagasta earthquake is considered, the area of significant deformation should not extend much outside the coastal range, nor should the area affected by subduction erosion. Consequently, the Chilean Precordillera and the Preandean Depression, and, with less probability, the Central Depression, should be affected mainly by the interseismic process of compressive strain accumulation. Hence, the transition between the extensional regime in the Coastal Cordillera (present study) and compressional tectonics in the Preandean Depression (Jolley *et al.* 1990) may be related to the eastward dying out of the mechanisms which promote extension in the west. Indeed, the Central Depression appears to be the transitional zone, a neutral zone as proposed by Mortimer & Saric (1975).

Estimation of the recurrence time of normal faulting earthquakes in the Coastal Cordillera

In order to estimate the recurrence time of normal faulting in the Coastal Cordillera we calculated the total cumulative area of scarps associated with normal faults in the studied area (Fig. 2). Cumulative scarps were roughly measured on 1:50 000 topographic maps. A total surface of 100 km^2 was obtained. Topographic scarps represent only the exposed (and eroded) parts of the total fault offset generated by repeated faulting. Hangingwall subsidence associated with normal faults produces half-grabens which fill with erosional and alluvial sediments, and, as a result, a large portion of the offset is hidden. Taking a conservative ratio of 1:1 between the exposed and hidden parts of the scarps, the surface corresponding to normal fault offset in the area would be 200 km^2. Representative rupture lengths and displacements associated with a magnitude 7 earthquake may be 40 km and 1.5 m. A magnitude 6 earthquake may typically have a rupture length of 10 km and a displacement of 0.6 m. Therefore, a magnitude 7 earthquake produces $\approx$0.06 km^2 of fault surface, whereas a magnitude 6 event creates 0.006 km^2. Since we are interested only in a first-order estimate of recurrence time, we will consider the unrealistic situation where only earthquakes of magnitude 7, or alternatively, of magnitude 6, occur. About 3300 events of magnitude 7 or 33 300 events of magnitude 6 are necessary to produce the 200 km^2 of surface rupture. Assuming a uniform rate of fault activity since 19 Ma, which corresponds to the lower bound given by Hervé (1987b), the recurrence time of magnitude 7 and 6 earthquakes in the area would be 5700 and 570 years, respectively. Large subduction earthquakes in northernmost Chile have a recurrence time of the order of 100–150 years (Comte & Pardo 1991). The comparison between the average recurrence times for continental and subduction events suggests that several large subduction earthquakes should occur in order to raise extensional deviatoric stresses enough for a magnitude 6 normal faulting event in this part of the Coastal Cordillera. Also, several tens of such subduction events should occur before the occurrence of a magnitude 7 normal faulting crustal earthquake. If, on the other hand, the distribution of faulting activity in time and space is strongly heterogeneous, as is suggested by the observation of a higher density of fresh ruptures between 23°S and 24°S, a much higher seismic hazard may exist locally.

CONCLUSIONS

Numerous fresh ruptures, especially between 23°S and 24 S, provide clear indications of moderate to large continental earthquakes in the late Quaternary. Long-term aridity has favoured the preservation of scarps. Strong contrasts in desert varnish (patina) between the exposed fault planes and the ground surface indicate the recent age of some ruptures. A number of faults associated with large cumulative scarps appear now to be less active, though isolated reactivation of old faults may occur after a long period of inactivity.

The long-term average uplift rate for the Neogene to Present in the Coastal Cordillera and in the Central Depression is estimated to be in between 0.05 and 0.1 mm yr^{-1}. Quaternary uplift rates obtained from marine terraces are in agreement with a long-term value of 0.05 mm yr^{-1} in Antofagasta Bay, but higher values, around 0.2 mm yr^{-1}, were found within the Mejillones Peninsula and along the coast further north. This is possibly due to a change in subduction regime, corresponding to a higher seismic coupling between the plates north of 23°S $-$24°S.

Neotectonic observations indicate that the coastal area of northern Chile, comprising both the Coastal Cordillera between 22.5°S and 24.5°S and the Mejillones Peninsula, are under E–W extension. Normal faults oriented approximately N–S and dipping towards the east predominate. These faults, whose cumulative scarps may reach a height of several hundred metres, are responsible for the half-graben structures widely observed in the area of study. Strike-slip components are also observed, with moderate horizontal offsets, no larger than one to two tens of metres. The sense of shear, and the ratio between vertical and horizontal offsets, vary coherently with the fault azimuth, compatible with a regional stress tensor corresponding to E–W extension. Recent kinematics along the Atacama Fault System, including the Atacama Fault itself, are controlled by this stress regime. Our observations confirm the existence of left-lateral displacements along the Salar del Carmen Fault (Atacama Fault NE of Antofagasta), a sense of strike-slip motion that was first reported by Armijo & Thiele (1990). However, we find the evidence presented by Armijo & Thiele (1990) for 60–100 m left-lateral offsets along the Salar del Carmen Fault unconvincing. In our opinion there is no clear evidence of large horizontal offsets (several tens of metres or more) along the Atacama Fault. On the other hand, the cumulative scarps along some segments of the Atacama Fault reach a height of several hundred metres. Our observations indicate that the Salar del Carmen Fault is a segmented east-dipping normal fault, frequently associated with antithetic secondary faults in the alluvial fans, with a local left-lateral component which may be as large as the vertical component on the most northeasterly oriented segments. At a regional scale, some of the faults, in particular the Atacama Fault, may appear continuous and linear because they were formed as strike-slip faults in the Mesozoic. When reactivated in the Tertiary and in Recent times under E–W extension, these faults were probably segmented, although they preserved an

unusually steep dip for normal faults. The cliff dipping seawards which bounds the Coastal Cordillera is not an active fault scarp.

Neotectonic observations do not provide evidence of strain partitioning along the margin. The Atacama Fault, at least in the Antofagasta region, is not a dextral fault as predicted by models of strain partitioning. The small left-lateral component of displacement observed and the strike-slip motion predicted by the convergence obliquity along the Atacama Fault are in opposite senses. This occurs because the predominant stress regime in the coastal region is not compressional, as may be expected in a convergent environment, but extensional. The left-lateral strike-slip component observed along the Atacama Fault (Salar del Carmen segment) does not mean that the coastal range is submitted to a different strain regime than that of the Mejillones Peninsula, a regime which would be related to the bending of the Andean orogen, as proposed by Armijo & Thiele (1990). This sinistral component is just a consequence of the extensional stress regime prevailing in the peninsular–coastal range area. Morphology and surface faulting in the outer forearc (offshore margin and Coastal Cordillera) suggest broad-scale flexure tectonics. Normal faulting exerts a strong control on surface topography at a relatively small wavelength, which is superposed on a regional uplift of 1000–1500 m. The long-wavelength morphology of the outer forearc reflects the broad-scale flexure, which may be controlled by offshore subsidence caused by subduction erosion near the trench, and by onshore uplift produced by underplating of low-density eroded material beneath the Coastal Cordillera.

The M_w=8.0 Antofagasta earthquake of 1995 July 30 showed how a large subduction earthquake produces E–W extension in the coastal region, in agreement with the regional stress tensor determined from neotectonic data. It also showed how crustal faulting may be triggered by large subduction earthquakes.

Although surface tectonics in the Mejillones Peninsula are shown to be controlled by large normal faults, the origin and deep structure of the peninsula remain an unresolved matter. As suggested by the available bathymetric data, a west-dipping normal fault bounding the peninsula to the west may have played some role in the peninsula uplift. A predominant role has been proposed for this fault (Armijo & Thiele 1990). However, it has been reported that the very regular spacing of Pleistocene shorelines on the Mejillones Peninsula lowland is more consistent with a deep-seated mechanism of uplift than with episodic tectonic movements (Ortlieb 1993). The subduction of an aseismic ridge has been proposed (Hartley & Jolley 1995), but the evidence is not as clear as in the case of the Nazca Ridge in Central Peru. Seismological data suggest that the Mejillones Peninsula is the surface expression of a barrier which blocked the propagation of the rupture of the 1995 Antofagasta earthquake towards the north. Conversely, this barrier may be an asperity to be broken during a future large subduction earthquake. This may occur when the large 1877 seismic gap of northernmost Chile is reactivated.

The important concentration of Tertiary to Recent extensional tectonics observed in the coastal area around the latitude of Antofagasta may be due to a combination of several factors: (1) a very important fault system, the Atacama Fault System, oriented roughly perpendicular to the Tertiary to Recent extension, was inherited from the Mesozoic; (2) large subduction earthquakes occur; (3) the coastal region is at the correct distance from the trench to be under extension; (4) strong subduction erosion and underplating seem to be operating in the area; and (5) tectonic scarps are well preserved thanks to the extreme aridity of the desert. Extensional structures may be mainly located offshore north of Iquique (20°S) since the distance between the trench and the coast increases northwards. Decreasing subduction erosion, together with stronger surface erosion on the continent, may be the determining factors explaining the absence of observed active extensional tectonics along the coast south of 26°S.

It is proposed that the state of stress in the outer forearc has a strong time-dependent component which is linked to the seismic cycle in the subduction zone. The apparent contradiction between observations of numerous recent surface ruptures and the absence of seismicity in the upper crust is explained by a process of episodic extensional deviatoric stress build-up. One of the permanent components of this extensional stress regime in the outer forearc is thought to be caused by subduction erosion near the trench and possibly by underplating beneath the Coastal Cordillera. Large subduction earthquakes contribute to the extensional regime because they produce coseismic E–W extension in the coastal area. Extensional deviatoric stresses should be reduced by interseismic contraction of the whole forearc during the period separating subduction earthquakes, as documented in several subduction zones worldwide. This interseismic contraction is related to ongoing slow steady plate motion while the plate interface is locked at shallow depth. If the balance between coseismic extension and interseismic contraction is in favour of extension in the outer forearc, extensional deviatoric stresses will accumulate over repeated seismic cycles. Eventually, the increment of extension associated with a large subduction earthquake will cause the Coulomb failure criterion to be fulfilled on a specific crustal fault. If failure is large enough, it may produce a visible fresh scarp at the surface. On the other hand, contraction in a general extensional stress regime means a departure from failure conditions, and faults in the outer forearc will remain aseismic during the period separating two large subduction earthquakes, in agreement with microseismic observations.

ACKNOWLEDGMENTS

This work has been supported by a grant from ORSTOM and by the ECOS program of cooperation between the Ministry of Foreign Affairs (France) and CONICYT (Chile). Partial financing has been given by the National Institute of Sciences of the Universe (INSU) in France, through the PNRN program. The authors are grateful to L. Ortlieb for his help concerning marine terraces in the Antofagasta region. We thank Peter Molnar and an anonymous reviewer for improving the manuscript with constructive criticisms and helpful discussions.

REFERENCES

Aki, K. & Richards, P.G., 1980. *Quantitative seismology: Theory and Methods*, Vol. 1, W.H. Freeman and Company, San Francisco, CA.

Arabasz, W.J., 1971. Geological and geophysical studies of the Atacama fault zone in Northern Chile, *PhD thesis*, California Institute of Technology, Pasadena, CA.

Armijo, R. & Thiele, R., 1990. Active faulting in northern Chile: ramp stacking and lateral decoupling along a subduction plate boundary? *Earth planet. Sci. Lett.*, **98**, 40–61.

Armijo, R., Carey, E. & Cisternas, A., 1982. The inverse problem in neotectonics and the separation of tectonic phases, *Tectonophysics*, **82**, 145–160.

Barrientos, S.E. & Ward, S.N., 1990. The 1960 Chile earthquake: coseismic slip from surface deformation, *Geophys. J. Int.*, **103**, 589–598.

Bott, M.H.P., 1959. The mechanics of oblique-slip faulting, *Geol. Mag.*, **96**, 109–117.

Bott, M.H.P., Waghorn, G.D. & Whittaker, A., 1989. Plate boundary forces at subduction zones and trench-arc compression, *Tectonophysics*, **170**, 1–15.

Brown, M., Diáz, F. & Grocott, J., 1993. Displacement history of the Atacama fault system 25°00'S–27°00'S, northern Chile, *Geol. Soc. Am. Bull.*, **105**, 1165–1174.

Coira, B., Davidson, J., Mpodozis, C. & Ramos, V., 1982. Tectonic and magmatic evolution of the Andes of northern Argentina and Chile, *Earth Sci. Rev.*, **18**, 303–332.

Comte, D. & Pardo, M., 1991. Reappraisal of great historical earthquakes in the northern Chile and southern Peru seismic gaps, *Natural Hazards*, **4**, 23–44.

Comte, D., Pardo, M., Dorbath, L., Dorbath, C., Haessler, H., Rivera, L., Cisternas, A. & Ponce, L., 1994. Determination of seismogenic interplate contact zone and crustal seismicity around Antofagasta, northern Chile, using local data, *Geophys. J. Int.*, **116**, 553–561.

Delouis, B., 1996. Subduction et déformation continentale au Nord-Chili, *PhD thesis*, Université Louis Pasteur, Strasbourg.

Delouis, B., Cisternas, A., Dorbath, L., Rivera, L. & Kausel, E., 1996. The Andean subduction zone between 22 and 25°S (northern Chile): precise geometry and state of stress, *Tectonophysics*, **259**, 81–100.

Delouis, B. *et al.*, 1997. The Mw=8.0 Antofagasta (Northern Chile) earthquake of July 30, 1995. a precursor to the end of the 1877 gap, *Bull. seism. Soc. Am.*, **87**, 427–445.

Dewey, J.F. & Lamb, S.H., 1992. Active tectonics of the Andes, *Tectonophysics*, **205**, 79–95.

Fitch, T.J. & Scholz, C.H., 1971. Mechanism of underthrusting in southwest Japan: A model of convergent plate interactions, *J. geophys. Res.*, **76**, 7260–7291.

Hartley, A.J. & Jolley, E.J., 1995. Tectonic implications of Late Cenozoic sedimentation from the Coastal Cordillera of northern Chile (22–24°S), *J. geol. Soc. Lond.* **152**, 51–63.

Hervé, M., 1987a. Movimiento sinistral en el Cretacico inferior de la zona de Falla Atacama al norte de Paposo (24°S), Chile, *Rev. Geol. Chile*, **31**, 37–42.

Hervé, M., 1987b. Movimiento normal de la Falla Paposo, zona de Falla Atacama, en el Mioceno, Chile, *Rev. Geol. Chile*, **31**, 31–36.

Jolley, E.J., Turner, P., Williams, G.D., Hartley, A.J. & Flint, S., 1990. Sedimentological response of an alluvial system to Neogene thrust tectonics, Atacama Desert, northern Chile, *J. geol. Soc. Lond.*, **147**, 769–784.

Kanamori, H. & Anderson, D.L., 1975. Theoretical basis of some empirical relations in seismology, *Bull. seism. Soc. Am.*, **65**, 1073–1095.

King, G.C.P, Stein, R. & Rundle, J.B., 1988. The growth of geological structures by repeated earthquakes 1. Conceptual framework, *J. geophys. Res.*, **93**, 13 307–13 318.

King, G.C.P., Stein, R. & Lin, J., 1994. Static stress changes and triggering of earthquakes, *Bull. seism. Soc. Am.*, **84**, 935–953.

Lallemand, S.E., Schnürle, P. & Malavielle, J., 1994. Coulomb theory applied to accretionary and nonaccretionary wedges: possible causes for tectonic erosion and/or frontal accretion, *J. geophys. Res.*, **99**, 12 033–12 055.

Leonard, E.M. & Wehmiller, 1991. Geochronology of marine terraces at Caleta Michilla, northern Chile; implications for Late Pleistocene and Holocene uplift, *Rev. Geol. Chile*, **18**, 81–86.

Mansinha, L. & Smylie, D.E., 1971. The displacement field of inclined faults, *Bull. seism. Soc. Am.*, **61**, 1433–1440.

Martinez, E. & Niemeyer, H., 1982. Depositos marinos aterrazados del Plioceno superior en la ciudad de Antofagasta, su relacion con la Falla de Atacama, *3° congreso Chileno*, Concepcion.

Mogi, K., 1970. Recent horizontal deformation of the earth's crust and tectonic activity in Japan, *Bull. Earthq. Res. Inst., University of Tokyo*, **48**, 413–430.

Mortimer, C., 1980. Drainage evolution in the Atacama desert of northernmost Chile, *Rev. Geol. Chile*, **11**, 3–28.

Mortimer, C. & Saric, N., 1975. Cenozoic studies in northernmost Chile, *Geol. Runds.*, **64**, 395–420.

Naranjo, J.A., 1987. Interpretation de la actividad Cenozoica superior a lo largo de la zona de Falla Atacama, norte de Chile, *Rev. Geol. Chile*, **31**, 43–55.

Naranjo, J.A., Hervé, F., Prieto, X. & Munizaga, F., 1984. Actividad Cretacica de la Falla Atacama al este de Chanaral: Milonitizacion y plutonismo, *Communicaciones*, **34**, 57–66, Department of Geology, University of Chile, Santiago.

Okada, A., 1971. On the neotectonics of the Atacama fault zone region – preliminary notes on Late Cenozoic faulting and geomorphic development of the Coast Range of northern Chile, *Bull. Dept Geogr., University of Tokyo*, **3**, 47–65.

Ortlieb, L., 1993. Vertical motions inferred from Pleistocene shoreline elevations in Mejillones Peninsula, northern Chile: some reassessments, *ISAG 93, Andean Geodynamics*, ORSTOM/University of Oxford, Oxford (UK), 21–23 September, 1993, extended abstract vol., pp. 155–158.

Ortlieb, L., Ghaleb, B., Hillaire-Marcel, C. & Pichet, P., 1993. Deformacion de la linea de costa del ultimo interglacial en la region de Antofagasta, N de Chile, Int. workshop 'The Quaternary of Chile', *Vth meeting of the IGCP Proj. 281 'Climas Cuaternarios de America del Sur'*, Santiago, abstract vol., p. 25.

Ortlieb, L., Ghaleb, B., Goy, J-L., Zazo, C. & Thiele, R., 1994. Terrazas marinas Pleistocenas del area de Hornitos (IIda Region): nuevos estudios morfoestratigraficos y neotectonicos en el Norte Grande de Chile, *7° Congreso Geologico Chileno*, University of de Concepcion, abstract vol., pp. 356–360.

Ortlieb, L., Barrientos, S., Ruegg, J.C., Guzman, N. & Lavenu, A., 1995. Coseismic coastal uplift during the 1995 Antofagasta earthquake. *I.G.C.P. project 367: Late Quaternary coastal records of rapid change*, IInd Annual Meeting, Antofagsta, Chile, Abstract vol., pp. 54–57.

Ortlieb, L., Goy, J-L., Zazo, C., Hillaire-Marcel, C., Ghaleb, B., Guzman, N. & Thiele, R., 1996. Quaternary morphostratigraphy and vertical deformation in Mejillones Peninsula, northern Chile, *ISAG 96*, ORSTOM/Géosciences Rennes, Saint Malo, France, Extended abstract vol., pp. 211–214.

Pardo-Casas, F. & Molnar, P., 1987. Relative motion of the Nazca (Farallon) and South American plates since Late Cretaceous time, *Tectonics*, **6**, 233–248.

Paskoff, R., 1980. Late Cenozoic crustal movements and sea level variations in the coastal area of Northern Chile. in *Earth Rheology, Isostasy and Eustasy*, ed. Morner, N.A., pp. 487–495, Wiley, New York, NY.

Paskoff, R. & Naranjo, J.A., 1983. Formation et évolution du piémont andin dans le désert du Nord du Chili (18–21° latitude Sud) pendant le Cénozoic supérieur, *C. R. Acad. Sci. Paris*, **297**, 743–748.

Plafker, G. & Savage, J.C., 1970. Mechanism of the Chilean Earthquakes of May 21 and 22, 1960, *Geol. Soc. Am. Bull.*, **81**, 1001–1030.

Radtke, U., 1987. Marine terraces in Chile (22°–32°S), Geomorphology, chronostratigraphy and neotectonics: Preliminary results, II. *Quat. South America Antarctic Peninsula*, **5**, 239–256.

Ratusny, A. & Radtke, U., 1988. Jüngere ergebnisse küstenmorphologischer untersuchungen im' grossen norden' Chiles, *Hamburger Geographische Studien*, **44**, 31–46.

Reutter, K-J., Giese, P., Gotze, H-J., Scheuber, E., Schwab, K., Schwarz, G. & Wigger, P., 1988. Structure and crustal development of the Central Andes between 21° and 25°S, *Lecture Notes in Earth Sciences,* vol. 17, *The Southern Central Andes,* pp. 231–261, eds Bahlburg, H., Breitkreuz, Ch., Giese, P., Springer-Verlag, Berlin.

Ruegg, J.C. *et al.*, 1996. The Mw=8.1 Antofagasta (North Chile) Earthquake of July 30, 1995. First results from teleseismic and geodetic data, *Geophys. Res. Lett.*, **23**, 917–920.

Rutland, R.W., 1971. Andean orogeny and ocean floor spreading, *Nature*, **223**, 252- 255.

Savage, J., 1980. Dislocations in seismology, in *Dislocations in Solids*, ed Navarro, F.R.N., North-Holland Publishing Co, Amsterdam.

Savage, J.C., Lisowski, M. & Prescott, W.H., 1991. Strain accumulation in western Washington, *J. geophys. Res.*, **96**, 14 493–14 507.

Scheuber, E. & Andriessen, A.M., 1990. The kinematics and geodynamic significance of the Atacama fault zone, northern Chile, *J. struct. Geol.*, **12**, 243–257.

Scheuber, E. & Reutter, K-J., 1992. Magmatic arc tectonics in the Central Andes between 21° and 25°S, *Tectonophysics*, **205**, 127–140.

Schmitz, M., 1994. A balanced model of the southern Central Andes, *Tectonics*, **13**, 484–492.

Schweller, W.J., Kulm, L.D. & Prince, R.A., 1981. Tectonics, structure, and sedimentary framework of the Peru-Chile Trench, *Geol. Soc. Am. Mem.*, **154**, 323–349.

Simpson, D.W., 1986. Triggered earthquakes, *Ann. Rev. Earth planet. Sci.*, **14**, 21–42.

Stern, C.R., 1991. Role of subduction erosion in the generation of Andean magmas, *Geology*, **19**, 78–81.

Tosdal, R.M., Clark, A.H. & Farrar, E., 1984. Cenozoic polyphase landscape and tectonic evolution of the Cordillera Occidental, southernmost Peru, *Geol. Soc. Am. Bull.*, **95**, 1318–1332.

von Huene, R. & Lallemand, S., 1990. Tectonic erosion along the Japan and Peru convergent margins, *Geol. Soc. Am. Bull.*, **102**, 704–720, 1990.

von Huene, R. & Scholl, D.W., 1991. Observations at convergent margins concerning sediment subduction, subduction erosion, and the growth of continental crust, *Rev. Geophys.*, **29**, 279–316.

Walcott, R.I., 1978. Geodetic strains and large earthquakes in the axial tectonic belt of north Island, New Zealand, *J. geophys. Res.*, **83**, 1978.

Whittaker, A., Bott, M.H.P. & Waghorn, G.D., 1992. Stresses and plate boundary forces associated with subduction plate margins, *J. geophys. Res.*, **97**, 11 933–11 944.

Wigger, P.J. *et al.*, 1994. Variation in the crustal structure of the southern Central Andes deduced from seismic refraction investigations, in *Tectonics of the Southern Central Andes,* pp. 23–48, eds Reutter, K.J., Scheuber, E. & Wigger, P.J., Springer-Verlag, Berlin.